Role of Eg5 regulation and motor properties in bipolar spindle assembly in Xenopus laevis egg extract

Julie Cahu

THESE DE DOCTORAT
DE L'UNIVERSITE PIERRE ET MARIE CURIE
ET DU LABORATOIRE EUROPEEN DE BIOLOGIE MOLECULAIRE

Spécialité:
Biologie Cellulaire

Présentée par:
Julie Cahu

Pour obtenir le grade de
DOCTEUR de l'UNIVERSITE PIERRE ET MARIE CURIE

Sujet de thèse:

Rôle de la régulation d'Eg5 et de ses propriétés motrices lors de la formation du fuseau mitotique dans l'extrait d'œuf de *Xenopus laevis*

Soutenue le ……

Devant le jury composé de:

Dr. Thomas SURREY	**Directeur de thèse**
Dr. Ariane ABRIEU	**Rapporteur**
Dr. Isabelle ARNAL	**Rapporteur**
Dr. Patricia BASSEREAU	**Examinateur**
Dr. Damian BRUNNER	**Examinateur**
Pr. Philippe DENOULET	**Examinateur**
Dr. Franck PEREZ	**Examinateur**

Acknowledgements

There are many people, without whom this work could not have been conducted and I would like to thank them. Since my lucidity decreases as my lack of sleep increases, I want to apologize for the persons that I might have forgotten.

First, I want to thank Thomas, who gave me the opportunity to do my PhD in his lab. Thomas' door was always opened. Coming to the lab every morning was not so difficult because of the good atmosphere that we are having. Therefore, I want to thank all the Surrey's lab members present and formal: my friend Peter, the irreplaceable Mathias, the smiley Aurelien, the nuddle cooker Henry, the philosopher Christian, the hairdresser expert Marianne, Ivo and Martina, whom I don't know very much, my ex bench mate Arne, and Jan. A special thank is going to Steffi, Jacques, and Jovanna, who were closely implicated in the project.

Moreover, I'm very thankful to all the people on the fifth floor from the Karsenti's lab, especially Iva and Sonja, and from the Brunner's lab, in particular our swiss chocolate provider Damian. I also want to thank Maria and Dietrich from the Nedelec's lab, Kreso for taking so much care of the frogs, Christiane for being "mon rayon de soleil" and Irina.

I want to sincerely thank my TAC committee members: Philippe Denoulet, Eric Karsenti and Iain Mattaj for helpful discussions and advices.

I am also extremely grateful to my parents for sending me carambars and to my sister, who was of a great support.

Last but not least, I want to thank my friends, especially Mirana, without whom I could never have managed until the end. I'm also thankful to Stuart and Matthieu, to Marthe, Aspasia, Laurent, Maiwen and a special thank to BC Heidelberg.

Table of contents

1 Introduction

1.1 Cell cycle and cell division

1.1.1 The cell cycle

The cell cycle represents an ensemble of events during which a cell duplicates its material and splits it into two new cells. The cell cycle can be seen as a succession of two main phases: interphase, during which the cell duplicates its material and mitosis phase or M-phase, during which the material is split.

Most of the cells spend 90% of their cell cycle in interphase, which is subdivided into three consecutive phases: G1 (Gap1), S-phase (Synthesis phase) and G2 (Gap2). During interphase, the microtubule organizing center or centrosome duplicates at the transition G1-S-phase and the chromosomes replicate in S-phase.

On the other hand, nucleus and cytoplasm divide during M-phase, in processes known as mitosis and cytokinesis respectively. The switch between interphase and M-phase is triggered by the Mitotis Promoting Factor (MPF), which is composed of cyclin dependent kinase 1 (Cdk1) and cyclinB2 (Murray et al., 1989), (Murray and Kirschner, 1989). Cdks are kinases that activate proteins by phosphorylating them during M-phase. Cdk activity depends on their interaction with cyclins.

Biochemical studies of the cell cycle, and yet MPF discovery, have been facilitated by the development of open systems such as cell extracts.

For instance, the early embryonic cell cycle of *Xenopus laevis* is a succession of interphasic and mitotic states, which can be easily recapitulated *in vitro* by the use of *Xenopus* egg extracts (Fig. 1) (Masui, 1974) (Lohka and Masui, 1984). As a consequence, events of interphase and M-phase could be studied in details by means of these extracts. More particularly, they have allowed the biochemical and mechanical characterization of M-phase or cell division.

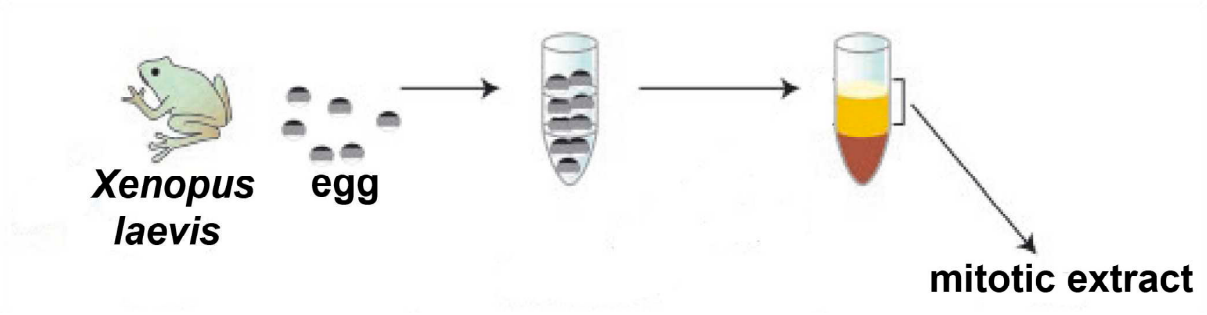

Figure 1: The *Xenopus* egg extract system. Adapted from (Karsenti and Vernos, 2001).

1.1.2 Cell division

Cell division is the process by which cells split and therefore is vital for unicellular and multicellular organisms. First, cell division underlies development of multicellular organisms. Second, it ensures the accurate segregation of the genetic material. As a matter of fact, chromosomal mis-segregation can lead to disorders such as Klinefelter, Turner or Down syndromes if it occurs during meiosis or sexual cell division, or to aneuploidy and cancer if it occurs during M-phase or somatic cell division. Third, it guaranties that each new cell receive only one centrosome. Indeed, aberrant centrosome number has been reported to contribute to aneuploidy (Wong and Stearns, 2003).

Both chromosome and centrosome segregations rely on the proper formation of the bipolar spindle during mitosis. The bipolar spindle results from the reorganization of rigid polymers, the microtubules, at mitosis onset.

Mitosis is subdivided in four phases: prophase, metaphase, anaphase and telophase.

In prophase, chromatin starts to condense into chromosomes followed by the disassembly of the interphasic radial array of microtubules. Two asters assemble from the newly duplicated centrosome and their microtubules start to interact, pushing them apart from each other.

During metaphase, the nuclear envelope breaks down, allowing microtubules to interact with chromosomes at specific sites called kinetochores (multi-protein complexes that assemble on centromeric DNA). Consequently, chromosomes congress and align at the metaphase plate. The bipolar metaphase spindle is established. At this stage, two classes of microtubules are distinguished in the spindle: kinetochore microtubules, which are in contact with kinetochores, and interpolar microtubules, which emanate from the opposite centrosomes or spindle poles (Fig. 2).

In anaphase, sister chromatids separate and are pulled towards their respective poles. The spindle starts to elongate moving the two spindle poles apart from each other.

In telophase, the separated chromatids have reached spindle poles and start to decondense. Mitosis is finished and cytokinesis begins. The cytoplasm is separated equally into two new cells, each containing one nucleus and one centrosome.

As a consequence, the accuracy of chromosome and centrosome segregations depends highly on spindle formation and function. The establishment of the bipolar spindle not only ensures the proper bipolar attachment of sister chromatids, hence the equal repartition of the genetic material to the daughter cells, but also drives chromatid and centrosome separations. Bipolar spindle assembly is therefore crucial for proper cell division.

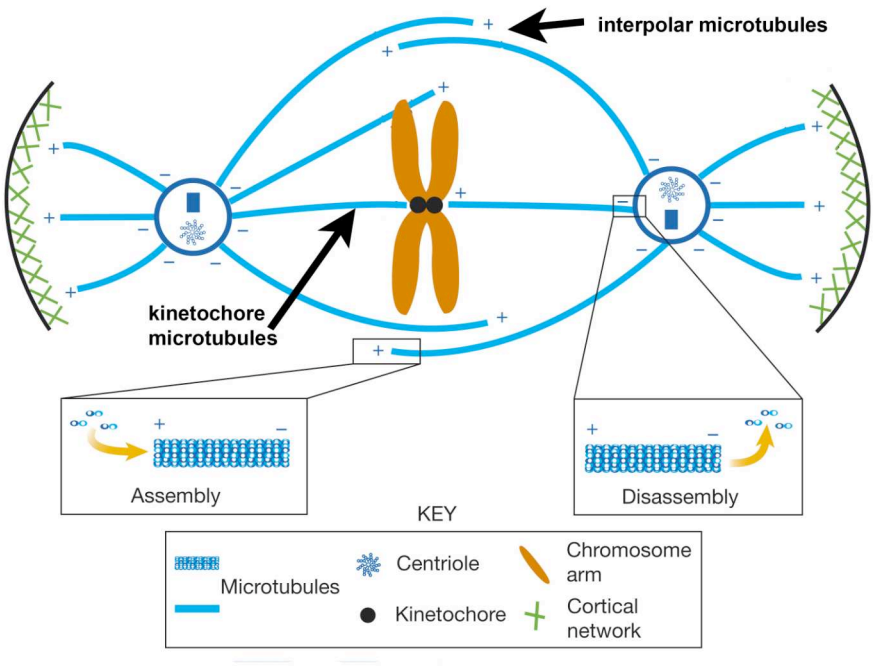

Figure 2: The metaphase spindle. Adapted from (Sharp et al., 2000).

1.2 The mitotic bipolar spindle

The bipolar spindle results from the dynamic organization of microtubules by microtubule associated proteins (MAPs) and molecular motors.

1.2.1 Microtubules

Microtubules are polymers arising from the polymerization of heterodimers of tubulin, α– and β– tubulin. Tubulin heterodimers associate head to tail into a protofilament. Usually 13 to

15 of these protofilaments assemble laterally in a sheet that finally closes forming a hollow cylindrical tube of 25nm diameter (Fig. 3A).

Microtubules are structurally and dynamically polarized filaments. Indeed, the tubulin heterodimers are arranged such that the β-tubulin monomer is exposed at the fast growing end or plus-end, while the α-tubulin monomer is at the more slowly growing end or minus-end. Microtubules alternate stochastically between polymerization and depolymerisation phases, which is referred to dynamic instability (Fig. 3B) (Mitchison and Kirschner, 1984). In addition, microtubules have been observed pausing. It has been suggested that microtubule dynamic instability is powered by guanosine triphosphate (GTP) hydrolysis. As microtubules polymerize, GTP on the β-tubulin is hydrolysed so that microtubules are almost only composed of GDP tubulin. However, the interactions between GDP tubulin subunits are weak. As a result the microtubule lattice is unstable and microtubule is ready to depolymerize. To prevent depolymerisation and allow growth, the microtubule plus-end is thought to be capped by β-tubulin subunits, which were delayed in their GTP hydrolysis, forming a stabilizing structure called the GTP-cap. Consequently, loss of the GTP cap would cause a rapid depolymerization of the microtubule.

Dynamic instability is thought to be of great importance in the behavior of microtubules *in vivo*. Indeed, dynamic instability would allow microtubules to explore more efficiently their surrounding space, which is an essential property for interphasic and mitotic microtubules. In interphase, microtubules, which form the cytoskeleton in addition to actin microfilaments and intermediate filaments, have to deliver vesicles or organelles in the cell cytoplasm.

In mitosis, microtubules have to catch chromosomes which is crucial for processes like spindle formation (Desai and Mitchison, 1997) .

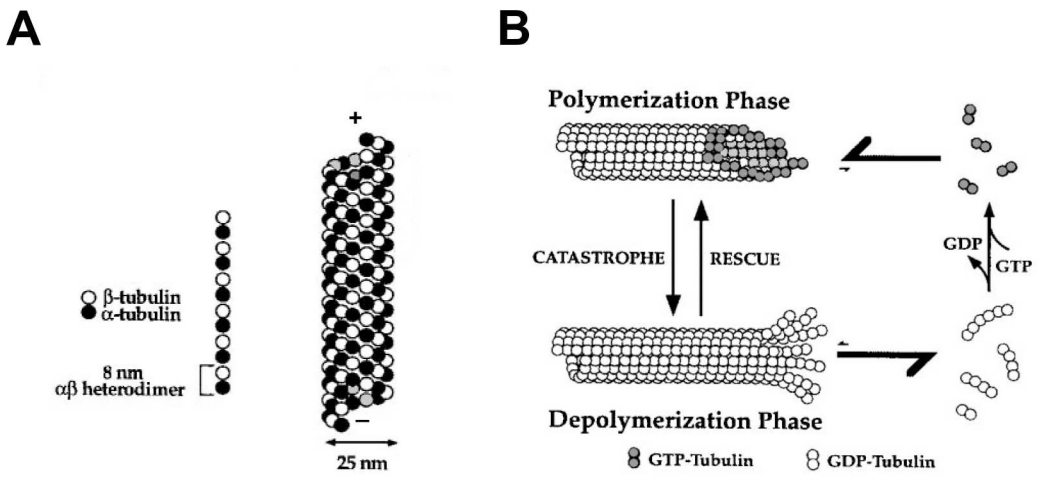

Figure 3: The microtubule. Adapted from (Desai and Mitchison, 1997). (A) Microtubule assembly. (B) Microtubule dynamic instability.

1.2.2 The microtubule associated proteins (MAPs)

To be able to catch chromosome, for example, microtubule dynamics must be somehow controlled, which is achieved by microtubule associated proteins (MAPs). MAPs are proteins that can bind in a nucleotide insensitive manner to the microtubule lattice.

MAPs can influence microtubule dynamics by stabilizing or destabilizing microtubules. MAPs that stabilize microtubules are often seen at microtubule plus-ends, such as EB1 or XMAP215. Although it is still not understood how plus-end tip proteins stabilize microtubules, two mechanisms of microtubule destabilization have been reported for MAPs. The first one is to sequester free tubulin subunits, such as Op18 or stathmin, while the second is to sever microtubule lattice, such as katanin (McNally and Vale, 1993). Katanin is an heterodimeric enzyme, which promotes microtubule disassembly by generating internal breaks within the microtubule lattice. This severing activity is cell cycle dependent and particularly high in mitosis (Vale, 1991) (McNally and Thomas, 1998).

Moreover, MAPs can also act as nucleating factors, for example TPX2.

MAPs are often found complexed with each other and their activity is also regulated, usually through phosphorylation.

1.2.3 The molecular motors

Like MAPs, molecular motors bind to microtubules and transduce chemical energy, provided by ATP hydrolysis, into kinetic energy for movement along microtubules. Microtubule-dependant molecular motors can be classified into two superfamilies: dyneins and kinesins.

1.2.3.1 The dynein superfamily

1.2.3.1.1 Classification and structure of dyneins

Dynein was first identified in 1965 by Gibbons (Gibbons, 1965a) (Gibbons, 1965b). Dynein is a microtubule minus-end motor and can be classified into two forms: axonemal and cytoplasmic dyneins.

Axonemal dynein has been implicated in cilia and flagella beating, whereas cytoplasmic dynein is involved in intracellular transport, mitosis, cell polarization and cell movement. Thereafter, we will only focus on cytoplasmic dynein.

Cytoplasmic dynein is a multi-subunit complex composed of variable numbers of heavy chains, intermediate chains, light intermediate chains and light chains. Dynein heavy chain interacts with microtubules via its stalk and contains the motor domain. The intermediate, light intermediate and light chains are thought to mostly interact with the cargo (Fig. 4).

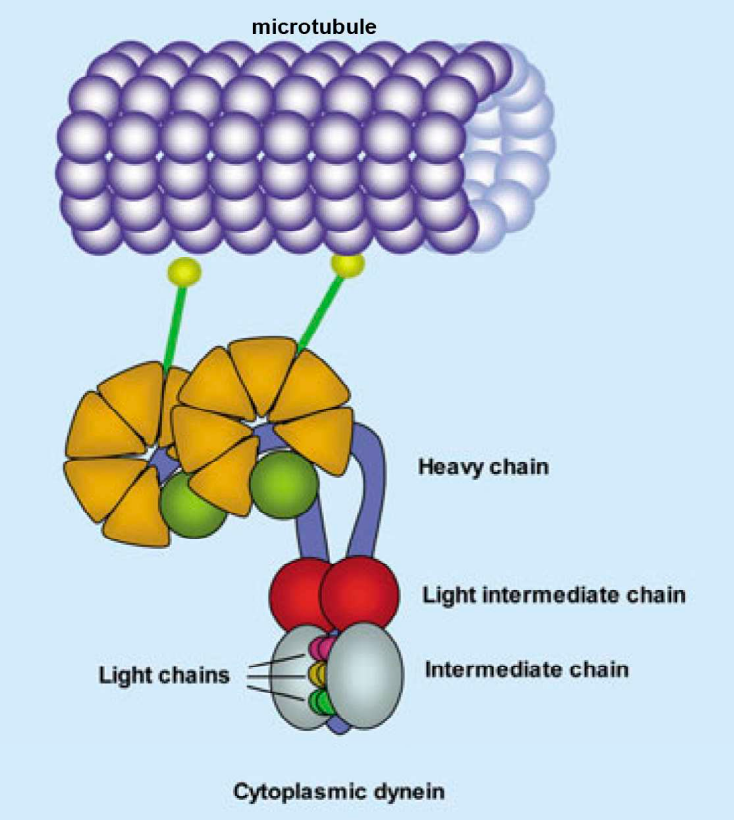

Figure 4: The cytoplasmic dynein. Adapted from (Hook and Vallee, 2006).

Dynein belongs to the AAA (ATPase Associated with diverse cellular Activities) class of proteins. As such, its motor domain is composed of seven globular domains arranged in a ring, out of which six are AAA domains. ATP hydrolysis at the AAA unit is transmitted to the microtubule binding stalk for force production leading to cargo transport along microtubules.

1.2.3.1.2 Motor properties of cytoplasmic dynein

In contrast to kinesins, the detailed mechanism of dynein stepping is unknown, probably due to its high molecular weight in the mega dalton range, which makes its study difficult. Although dynein alone is sufficient to drive microtubule gliding *in vitro*, addition of yet another multi-protein complex, dynactin, considerably enhances dynein motor properties.
Dynactin can interact *in vivo* and *in vitro* with dynein intermediate chain but can also directly bind microtubules via its $p150^{glued}$ subunit. This additional microtubule binding site of dynactin could explain the increase in dynein processivity *in vitro* (King and Schroer, 2000).
In addition, dynein has been proposed to function like a 'gear' as its step size decreases while its produced force increases under increasing load (Mallik et al., 2004).

1.2.3.1.3 Function and regulation of cytoplasmic dynein

Unlike kinesins, which have expanded and specialized in evolution, often resulting in 'one kinesin=one function', dynein completes its various functions by interacting with different accessory proteins.

First, the composition of dynein itself can be subjected to changes. Heterogeneity in dynein light intermediate chain number could lead to differential regulation of its motor domain. In this way, it has been reported that dynein intermediate chain could act as a negative regulator of the motor domain (Mallik and Gross, 2004).

As already mentioned, dynein can interact with dynactin, probably in a phosphorylation dependent manner. Formation of the dynein/dynactin complex is essential for dynein targeting and function. For example, dynein localization at the kinetochore is achieved through dynactin binding to ZW10, a kinetochore component. This ternary complex may be involved in a tension-sensitive checkpoint mechanism, which would delay anaphase if chromosome bipolar attachment is defective (Starr et al., 1998).

MAP-2 has also been reported to stimulate dynein detachment from microtubules, probably by interfering with dynein microtubule binding sites (Schroer, 1994).

1.2.3.2 The kinesin superfamily

1.2.3.2.1 Classification and structure of kinesins

The founding member of the kinesin superfamily was identified in 1985 by Vale *et al* (Vale et al., 1985) and Brady (Brady, 1985). The superfamily has now expanded and includes 14 subfamilies of kinesin-related proteins (KRP) (Lawrence et al., 2004) (Fig. 5). Each KRP shares a roughly 350 amino acid sequence that represents the motor domain. The motor domain, which contains the microtubule and the nucleotide binding sites, is usually followed by a stalk domain and a tail domain.

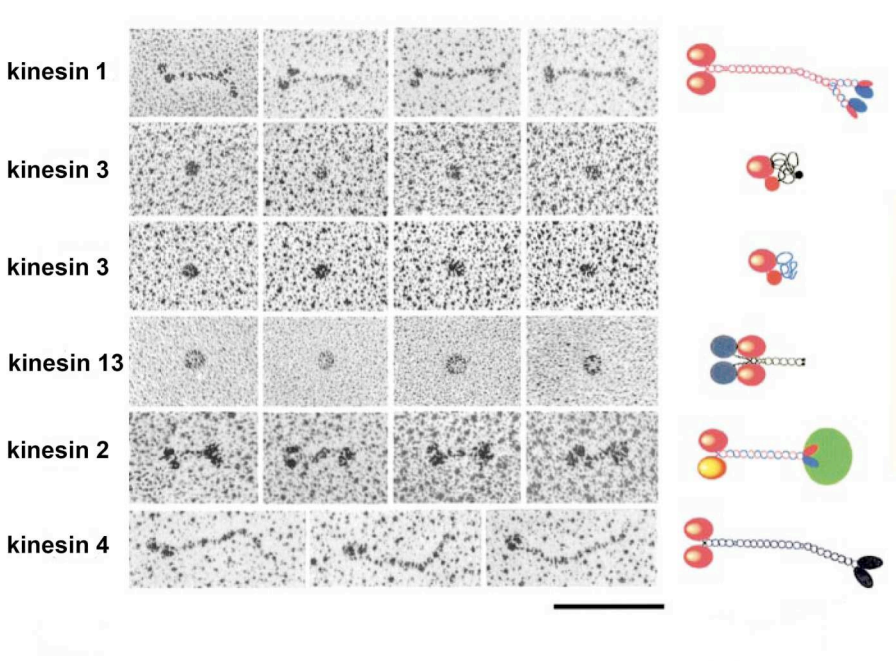

Figure 5: Example of members of the kinesin superfamily, as observed by low-angle rotary shadowing electron microscopy on the left and their schematic illustrations on the right. Scale bar is100nm. Adapted (Hirokawa, 1998).

However, not all KRPs possess a motor domain in the N terminus of their polypeptide sequence. Indeed, KRP motor domain can also be found at the C terminus or internally within their polypeptide sequence. Interestingly, KRP with a C terminus motor domain are microtubule minus-end directed motors, while KRP with an internal motor domain modulate microtubule dynamics.

As noticed, there is a correlation between KRPs directionality and their motor domain location. A region between the motor and the stalk domains, called the neck linker, has been shown to be involved in KRPs directionality (Sablin et al., 1998). Thus, the neck linker 'dictates' the orientation of the unbound motor domain so that it extends towards microtubules plus-ends for KRP with a N terminal motor domain, for example, initiating movement.

1.2.3.2.2 Motor properties of kinesins

The mechanism of movement of KRPs along microtubules varies between different KRPs and it seems that even the same KRP can switch occasionally between different modes of movement. Nevertheless, 3 categories of movement can be described for KRPs: processive movement, non-processive movement and diffusion.

A processive motor makes several steps before detaching from the microtubule. It is now well accepted that the hand-over-hand model, in which the release of the rearward head is tightly coupled with the binding of the forward head, can describe KRP processive movement. Succinctly, the forward head releases its adenosine diphosphate (ADP) upon microtubule binding. Subsequent ATP binding promotes docking of the flexible neck linker, "throwing" the rearward head in the front. The new forward head binds the microtubule. ATP hydrolysis occurs on the new rearward head followed by phosphate release and detachment. Thus, ADP release is catalyzed by KRP binding to the microtubule, whereas unbinding of KRPs from the microtubule requires ATP hydrolysis (Howard, 2001). The kinetic properties of the conventional kinesin, which belongs to the kinesin-1 subfamily, have been extensively studied: it moves along microtubules with a speed of 20μm/min, hydrolyses one ATP per step and makes on average 100 steps of 8nm, corresponding to a tubulin dimer, per run. Optical-trapping studies have also revealed that conventional kinesin can sustain hindering loads up to 6pN, with its velocity slowing down until the motor finally stalls (Valentine and Gilbert, 2007). Most of the KRPs studied so far move processively along microtubules (Fig. 6).

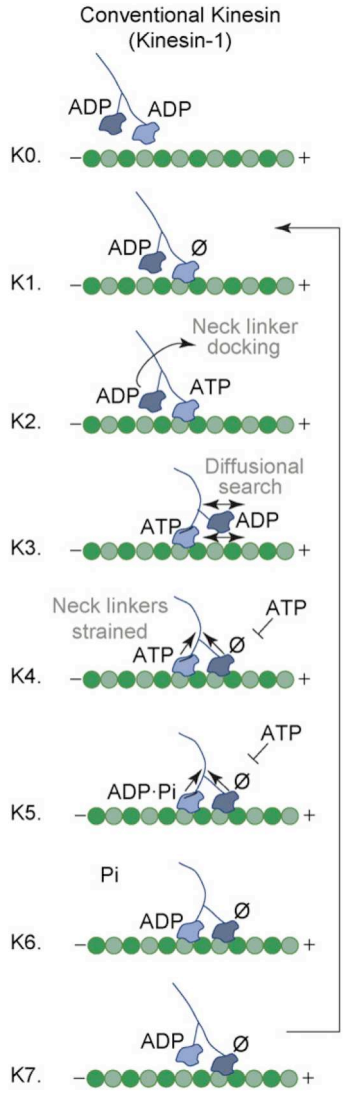

Figure 6: Stepping (K0-K7) model for kinesin. Adapted from (Valentine and Gilbert, 2007).

In contrast to processive KRPs, non-processive KRPs make only one step. Typically, non-processive KRPs bind to microtubules, hydrolyze one ATP and dissociate from the microtubule. Non-processive motors are thought to act cooperatively in an ensemble to perform their task. KIF1D, a plus-end directed KRP and Ncd, a dimeric minus-end directed KRP, have been shown to be non-processive (Endow and Barker, 2003).

Although different, processive and non-processive movements can be explained by a stepping mechanism that allows KRPs to move along microtubules. Surprisingly, KRPs with an internal motor domain do not move in a step-by-step fashion to reach microtubule ends but rather diffuse in an ATP independent mechanism. Instead of using their ability to generate movement via ATP hydrolysis, these KRPs, such as XKCM1, use ATP hydrolysis to depolymerize efficiently microtubules (Moore and Wordeman, 2004) (Walczak et al., 1996).

1.2.3.2.3 Function and regulation of kinesins

As there is a various number of KRPs with potentially different functions, the general function of the different KRPs subfamilies are listed in Table 1, without detailing each subfamily members.

Table 1: Functions of KRPs subfamilies. Adapted from (Mountain and Compton, 2000).

Subfamily	Directionality	General function	Members (non-exhaustive list)
Kinesin-1	plus-end	Non mitotic motor: cargo transport	DmKHC
Kinesin-2	plus-end	Non mitotic motor: anterograde transport in association with KAP3	KIF3A/3B, KRP85/95
Kinesin-3	plus-end	Non mitotic motor: cargo transport	KIF1
Kinesin-4	plus-end	Mitotic motor: microtubule/DNA attachment, chromosomes segregation Non mitotic motor: organelle transport	Kid, Xklp1, KIF4
Kinesin-5	plus-end	Mitotic motor: spindle bipolarity	bimC, Cin8, Kip1, Cut7, Eg5, Klp61F
Kinesin-6	plus-end	Mitotic motor: central spindle formation and cytokinesis	MKLP1, ZEN-4, CHO1, pavarotti
Kinesin-7	plus-end	Mitotic motor: microtubule/kinetochore attachment, chromosomes segregation	CENP-E
Kinesin-8	plus-end	Microtubule depolymerisation Nuclear migration	Kip3
Kinesin-13	No directed motility	Microtubule depolymerisation	MCAK, XKCM1, KIF2A
Kinesin-14	minus-end	Mitotic motor: microtubule cross-linking, opposition Kinesin-5	HSET, XCTK2, ncd, CHO2, KAR3

As described above, KRPs have different functions even within one subfamily. As a consequence, their tail domains have been postulated to encode ‘functional information’.

Indeed, regulatory elements like phosphorylation sites can be found in the tail domains of Eg5 (Sawin and Mitchison, 1995) and CENP-E (Liao et al., 1994) for example but also directly in the motor domain as for MKLP1. These regulatory elements often control KRP binding to microtubules as an ON/OFF switch. Other KRPs, like XCTK2, are regulated via their binding to an activator/repressor (Ems-McClung et al., 2004).

MKLP1 is probably the best example to illustrate the complexity of KRP regulation as it can be phosphorylated by two different kinases in two different residues. Indeed, in early mitosis, Cdk1/cyclinB phosphorylates the MKLP1 motor domain preventing its binding to spindle microtubules (Mishima et al., 2004). Upon anaphase as Cdk1 activity decreases, MKLP1 starts to assemble the central spindle by binding to microtubules. Once at the central spindle, the MKLP1 tail can be phosphorylated by Aurora B to allow proper completion of cytokinesis (Guse et al., 2005). Thus, MKLP1 is temporally and spatially regulated.

1.2.4 Spindle architecture

Spindle formation requires dynamic microtubules, MAPs and molecular motors but their mechanistical interplay is still not understood.

The first well accepted model formulated to describe spindle formation was the "search and capture" model (Kirschner and Mitchison, 1986). In this model, dynamic microtubules nucleated from the two centrosomes are stabilized and captured by kinetochores. Once the spindle axis is determined, connections between microtubules emanating from opposite poles are established. In this case, the two centrosomal asters act as drivers of spindle bipolarity.

However, bipolar spindles were also observed to form around chromatin beads, without centrosomes and kinetochore microtubules, suggesting that chromatin could also drive spindle bipolarity (Heald et al., 1996). Several studies have since demonstrated the existence of a gradient of a small GTPase in its GTP bound form, RanGTP, around chromatin (Kalab et al., 2002) (Kalab et al., 2006). Such a RanGTP gradient could give spatial cues for MAPs and molecular motors to assemble the spindle (Caudron et al., 2005). Bipolar spindles could arise from self-organization of microtubules around chromatin.

A new model emerged, in which bipolar spindle formation results from a combination of centrosomal search and capture and chromatin self organization.

Once established, the dynamic mitotic spindle has to be maintained for a certain period of time before anaphase onset. Spindle bipolarity maintenance is thought to be achieved by a "push and pull" mechanism. In such a mechanism, antagonistic microtubule-sliding motors

would be balanced to ensure spindle integrity. Two mitotic motors, Eg5 and XCTK2, have been shown to play an essential role. Both motors crosslink antiparallel microtubules in the interpolar region. However, Eg5 moving towards microtubule plus-ends would push the pole apart, while XCTK2 moving towards microtubule –ends would pull them together (Saunders and Hoyt, 1992) (Roof et al., 1992) (Sharp et al., 1999b) (Sharp et al., 1999a). Such opposing activity has also been described in a reduced systems, for example in aster formation (Mountain et al., 1999) (Surrey et al., 2001).

Recently, microtubule poleward flux has been suggested to be involved in spindle bipolarization. Microtubule poleward flux was first observed by Mitchison (Mitchison, 1989) and describes the continuous movement of spindle microtubules towards spindle poles during mitosis. Microtubule poleward flux has been reported to appear as monoaster spontaneously bipolarizes into spindle, suggesting that microtubule antiparallel organization, mediated by Eg5, is required for flux (Mitchison et al., 2004).

Hence, Eg5 plays an interesting and important role in the process of spindle formation in general and in spindle bipolarity in particular, which makes it interesting, in respect of cell division, for further investigation.

1.3 The *Xenopus* kinesin-5: XlEg5

1.3.1 Eg5 homologs

Xenopus laevis Eg5, XlEg5, was first identified by screening for mRNAs that are essential for the rapid and synchronous cell divisions occurring after fertilization in *Xenopus laevis* (Le Guellec et al., 1991). After sequence analysis, they found that XlEg5 shared homology with an *Aspergillus nidulans* KRP: BimC. XlEg5 is a mitotic KIN-N KRP and belongs to the kinesin-5 subfamily. It is well conserved from *A. nidulans* to *Homo Sapiens*, suggesting that it underlies an important role in mitotic events (Fig. 7).

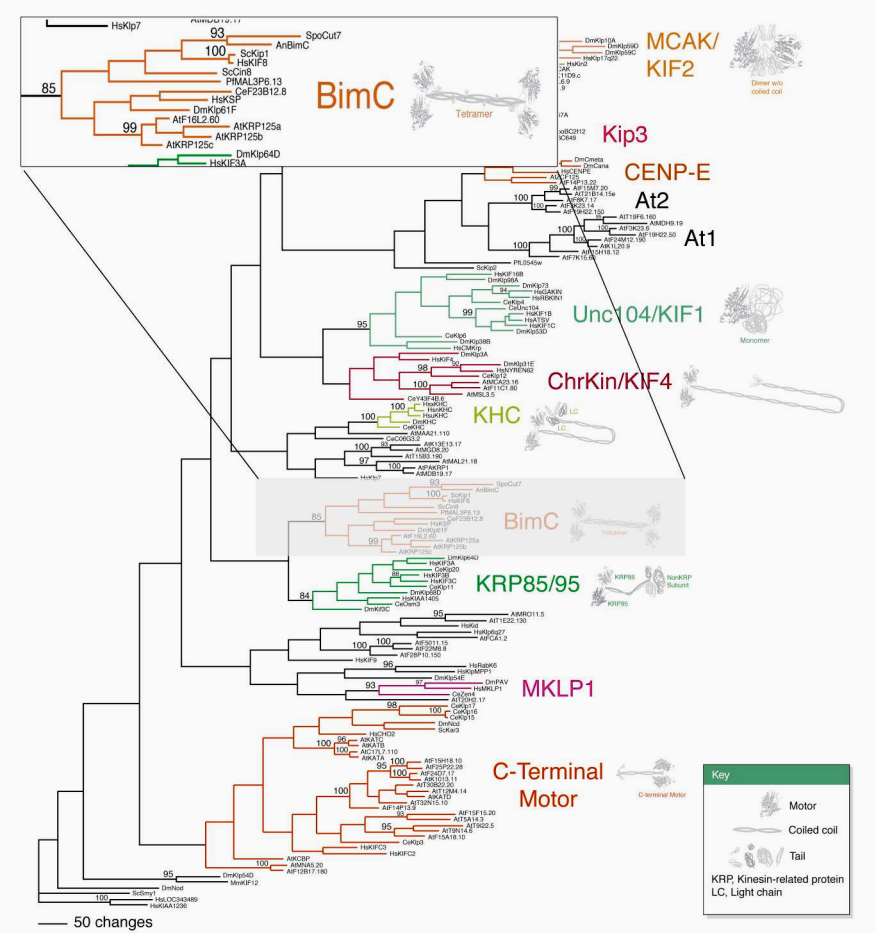

Figure 7: The kinesin 5 family members. Adapted from (Dagenbach and Endow, 2004).

In vertebrates, Kinesin-5 is found on spindle microtubules and at spindle poles on the metaphase spindle in mitosis. It has also been observed on interphase microtubules although this point is still under debate (Houliston et al., 1994) (Sawin and Mitchison, 1995).

1.3.2 Structure of Eg5

Interestingly, all the members of the kinesin-5 subfamily display the same unusual ultra-structure. Indeed, Eg5 is a tetramer whereas most of the KRP are dimers.

Eg5 homotetramer has a bipolar arrangement with motor domains at opposite ends. Kashina *et al* (Kashina et al., 1996a) (Kashina et al., 1996b) described it as an elongated structure with an overall length of 100nm on average, consisting of two globular domains of 25nm diameter connected by a central rod with a length of 65nm. Furthermore they observed that Eg5 could bind microtubules with one or both ends.

Another interesting feature was revealed by Turner *et al* (Turner et al., 2001) as they crystallized the Eg5 motor domain. In contrast to conventional kinesin, the Eg5 neck linker appears to be well ordered. This calls Eg5 stepping mechanism into question, as the flexibility of conventional kinesin neck linker was essential for its processivity.

1.3.3 Motor properties of Eg5 *in vitro*

Thanks to the development of single molecule assays, insight into Eg5 motor properties was gained and in particular the role of its unique neck linker configuration for its processivity. Eg5 processivity has remained for a long time under debate, whereas Eg5 plus-end directed microtubule gliding, with a velocity of 2μm/min, was clearly demonstrated (Sawin et al., 1992a). A study by Valentine *et al* (Valentine et al., 2006), using optical-trapping shed light on Eg5 processivity.

In this study, Valentine *et al* demonstrated that individual purified Eg5 dimers (hsEg5-513-5His) step processively along microtubules. Eg5 dimers make on average 8 steps per run (compared to 100 for conventional kinesin), with 1 step per tubulin dimer and one ATP hydrolysed per step (like conventional kinesin). Moreover, they showed that Eg5 velocity was less force-sensitive when compared to conventional kinesin. While kinesin velocity slows and stalls at high hindering loads, Eg5 dissociates from microtubules after a slight slowdown. Furthermore, they interpreted this low processivity as being a consequence of Eg5 rigid neck linker. In order that the Eg5 forward head binds ATP, Eg5 neck linker must undergo a conformational change from perpendicular to parallel with respect to the long axis of the motor core. Once this isomerisation has occurred and ATP has bound, the rearward head can move forward, initiating the processive run. This rearrangement of Eg5 neck linker was also described by Rosenfeld *et al* (Rosenfeld et al., 2005), and is believed to be slow: 0.5 - 1 s^{-1} (Valentine and Gilbert, 2007). This also suggests that unlike kinesin, for which stepping is limited by phosphate release, ATP hydrolysis is rate limiting for Eg5 stepping.

Recombinant Eg5 tetramer has also been reported to be processive by Kwok *et al*, who also described an additional diffusive component to Eg5 motility (Kwok et al., 2006). Eg5 diffusive behavior is ATP independent, in contrast to its directional stepping, and is favored when Eg5 is inhibited by monastrol (Crevel et al., 2004). Korneev *et al.* (Korneev et al., 2007) also confirmed that Eg5 tetramer is processive with an 8nm step size and an average of 10 steps per run, similar to Eg5 dimer. However, they reported that individual Eg5 tetramers are released at lower force compared to individual Eg5 dimers (respectively 2pN in low salt

buffer and 7pN in high salt buffer), suggesting that Eg5 load-dependent detachment could be regulated by the Eg5 tail.

These final evidences that Eg5 tetramer is processive corroborate and furthermore give a possible explanation to previous experiments such as those of Kapitein *et al* in which they observed that Eg5 tetramers crosslink, align and drive microtubules sliding relative to each other (Kapitein et al., 2005). This would have been difficult to explain for a non-processive motor as its probability of simultaneously binding two microtubules would be extremely low. One should also emphasize that this study was the first to directly show that Eg5 could crosslink parallel and slide antiparallel microtubules.

These studies have shed light on Eg5 *in vitro* motor properties, providing basis to understand Eg5 *in vivo* motor properties and in particular in relation to its function.

1.3.4 Function of Eg5 *in vivo*

1.3.4.1 Eg5 function in bipolar spindle formation and maintenance

The monopolar phenotype observed when the Eg5 inhibitor, monastrol, is added to BS-C-1 cells was further characterized by Kapoor *et al* (Kapoor et al., 2000). They concluded that monastrol inhibits centrosome separation, hence leading to monopolar spindles. This is consistent with previous data involving Eg5 in centrosome separation and consequently bipolar spindle formation, although these observations are still under debate in *Drosophila melanogaster* (Sharp et al., 1999b).

Interestingly, the role of Eg5 in bipolar spindle assembly seems to be evolutionarily conserved since it has been described in *A. nidulans* (Enos and Morris, 1990) in fission yeast (Hagan and Yanagida, 1990), in *Saccharomyces cerevisiae* 11 (Hoyt et al., 1992), in *Drosophila melanogaster* (Heck et al., 1993), in *Xenopus* (Sawin and Mitchison, 1995), in *Homo Sapiens* (Blangy et al., 1995). In addition to bipolar spindle assembly, Eg5 has also been implicated in bipolar spindle maintenance, probably in a "push and pull" mechanism, as addition of anti-Eg5 antibodies or monastrol disrupt preformed spindle in *Xenopus* egg extract (Sawin et al., 1992b) (Kapoor et al., 2000). Both bipolar spindle formation and maintenance intimately rely on Eg5 capacity to link interpolar microtubules together *in vivo* as described by Sharp *et al* (Sharp et al., 1999a), and remarkably reflect Eg5 *in vitro* motor properties (Kapitein et al., 2005).

This shows that Eg5 is absolutely essential for spindle bipolarity and therefore proper chromosome segregation in all eukaryotes except *Caenorhabditis elegans* (Saunders et al., 2007).

1.3.4.2 Eg5 function in microtubule poleward flux

It is no longer controversial that Eg5 also plays a role in microtubule poleward flux. Poleward flux is composed of 3 coordinated activities: microtubule minus-end depolymerization, microtubule translocation and microtubule plus-end polymerization (Kwok and Kapoor, 2007) (Rogers et al., 2005).

Spindle elongation rate and Eg5 microtubule sliding rate have been correlated (Shirasu-Hiza et al., 2004), suggesting that Eg5 is responsible for the 'microtubule translocation activity' of poleward flux. Eg5 involvement in microtubule poleward flux has also been reported in *Xenopus* egg extract (Miyamoto et al., 2004). Indeed, addition of Eg5 inhibitors inhibited spindle microtubule poleward flux in a dose-responsive manner, suggesting that flux is driven by an ensemble of non-processive Eg5. In addition, microtubules move poleward with a speed of 2μm/min in *Xenopus* egg extract 2,22μm/min in *Drosophila* S2 (Rogers et al., 2004), which is found to match Eg5 microtubule gliding speed *in vitro*. However, Eg5 is probably not the only flux driver as Eg5 independent poleward flux as been observed for kinetochore microtubules, which interestingly are organized in parallel arrays, in PtK1 cells (Cameron et al., 2006).

Since both spindle bipolarity and microtubule poleward flux clearly involve Eg5 antiparallel microtubule cross-linking and sliding activities, it is not surprising that spindle bipolarization itself relies on microtubule poleward flux, at least in *Xenopus* egg extract, as suggested by Mitchison *et al* (Mitchison et al., 2004).

1.3.4.3 Eg5 function in a potential spindle matrix

Owing to Eg5 intriguing localization to spindle poles, it was proposed earlier that Eg5 could be part of a "spindle matrix" (Sawin et al., 1992a). Thus Eg5 localization to minus-ends of microtubules would not depend on its motor activity as such. However, the existence of the matrix itself is still hypothetical as its composition, regulation and role are unknown. The current hypothesis proposes that such a matrix would help to stabilize, organize microtubules and serve as a stationary substrate against which motors could slide microtubules (Scholey et

al., 2001).

To date, many different proteins (*e.g.*: NuMa, skeletor) have been proposed to form or be part of the matrix. The best candidate so far is lamin B as it associates with the mitotic spindle, is nocodazole insensitive and retains a certain number of proteins involved in spindle formation such as Eg5 (Tsai et al., 2006). Moreover, another study also implicated Eg5 as being part of a spindle matrix (Kapoor and Mitchison, 2001).

As described above, the evidence for the matrix existence and thus, Eg5 being part of it, are rather poor. As a consequence, the actual role of Eg5 in the matrix remains unclear, in particular if the matrix is a non-microtubule based structure, raising the question of how the microtubule-dependant molecular motor Eg5 can bind to it.

1.3.5 Regulation of Eg5

1.3.5.1 Cdk1 phosphorylation of Eg5

All the members of the kinesin-5 subfamily possess a conserved sequence in their C-terminal part, called the "bimC box" (Heck et al., 1993). Interestingly, besides its location in the tail, the bimC box contains a highly conserved sequence: TGX-TPXK/RR (in Eg5 TGTTPQRR) with a Cdk1/cyclinB consensus site (underlined). As a consequence, it has been postulated that Cdk1 could phosphorylate Eg5 in its bimC box to regulate Eg5 function.

Indeed, expression of the mutant Eg5 T937A, in which Cdk1 phosphorylation is silenced, abolishes Eg5 localization to spindle microtubules but does not perturb spindle formation in a dominant negative fashion in HeLa cells and in *Xenopus* A6 cells (Blangy et al., 1995) (Sawin and Mitchison, 1995). In 2005, Goshima *et al* (Goshima and Vale, 2005) investigated Eg5 *Drosophila melanogaster* homolog, Klp61F, phosphorylation by Cdk1. By means of RNA interference, endogenous Klp61F was knocked down and replaced by Klp61F T933A, in which the conserved Cdk1 phosphorylation site was mutated. Klp61F T933A could not rescue spindle bipolarity, as most structures were monopolar spindles. They confirmed that Klp61F phosphorylation by Cdk1 is essential for Klp61F to interact with microtubules and therefore to function, explaining the monopolar spindle phenotype.

Surprisingly, mutation of the Eg5 Cdk1 phosphorylation site in the Eg5 homolog, Cut7, does not affect its association with the mitotic yeast spindle (Drummond and Hagan, 1998).

In addition, Eg5 phosphorylation by Cdk1 has also been reported to control Eg5 association with dynactin (Blangy et al., 1997).

1.3.5.2 Eg2 phosphorylation of Eg5

Another kinase, Aurora A or Eg2 in *Xenopus laevis*, has also been reported to phosphorylate Eg5 in *Xenopus* egg extract.

Eg2, which belongs to the AIRK kinase family, was shown to be involved in centrosome separation and bipolar spindle stability (Glover et al., 1995) (Giet and Prigent, 2000). The strong similarities between Eg2 and Eg5-depletion phenotypes suggest that both proteins might interact. Indeed, Eg2 can interact with Eg5 and furthermore can phosphorylate a truncated version of Eg5 in its stalk domain *in vitro* (Giet et al., 1999). Unfortunately, the Eg2 phosphorylation site of Eg5 still remains unidentified.

1.3.5.3 RanGTP regulation of Eg5

As previously mentioned, RanGTP stimulates spindle formation by changing microtubule dynamics and the balance of motor activities (Wilde et al., 2001). Microtubule seed movements were observed along microtubules of taxol induced-asters in *Xenopus* egg extract. Seeds movement was bidirectional, but a twofold increase in the number of seeds moving away from the center was found upon RanL43E addition (a constitutively active Ran bound to GTP). Furthermore, this movement was demonstrated to be Eg5 driven, which led to the conclusion that RanGTP increases the number of motile Eg5, probably by releasing it from the center of the aster. Moreover, no changes could be detected in Eg5 velocity upon RanGTP addition.

Another study (Silverman-Gavrila and Wilde, 2006) also reported that Eg5 is mis-localized in spindles formed in *Drosophila* embryos injected with a RanT24L (constitutively inactive Ran). Bipolar spindles formed in the presence of RanT24L are shorter than control spindles, which was also described in *Xenopus* egg extract (Carazo-Salas et al., 2001).

The fact that RanGTP might influence Eg5 properties is interesting in regards to its phosphorylation by Eg2. Indeed Eg2 kinase activity and thus spindle assembly is RanGTP dependent (Tsai et al., 2003). Therefore, RanGTP could activate Eg2 kinase, which in turn would phosphorylate Eg5 allowing spindle formation. In addition, Eg5 and Eg2 have been characterized as part of a complex involved in spindle formation (Koffa et al., 2006). However no increase in Eg5 phosphorylation is detected upon RanGTP addition in *Xenopus* egg extract (Wilde et al., 2001).

2 Motivation

Bipolar spindle assembly is an essential process of cell division, which success intimately depends on Eg5. As already reported, Eg5 regulation and motor properties are required for spindle formation. However, their relative contribution remains unclear and will therefore be addressed in this study.

On one hand, we will focus on Eg5 regulation by two kinases, Eg2 and Cdk1, which have been shown to phosphorylate Eg5. For this purpose, non-phosphorylatable mutants will be generated and their ability to assemble spindles will be tested by a depletion/add back experiments in *Xenopus* egg extract.

On the other hand, Eg5 motor properties will be examined by generating Eg5 chimeras, in which Eg5 motor domain will be replaced by other motor domains with distinct properties. To investigate whether these new motor properties can substitute for the Eg5 original ones, the ability of the Eg5 chimeras to form a bipolar spindle will be examined by a depletion/ add back experiment in *Xenopus* egg extract. In parallel, Eg5 motor properties will be directly assessed by means of a newly developed microtubule gliding assay in *Xenopus* egg extract.

3 Results

3.1 Role of Eg5 phosphorylation in bipolar spindle formation in *Xenopus* egg extract

3.1.1 Eg2 phosphorylates full length Eg5 at serine 543

3.1.1.1 Eg2 phosphorylates truncated GST-Eg5 at serine 543 *in vitro* and in mitotic egg extract

In order to identify a potential Eg2 phosphorylation site in the Eg5 sequence, full length Eg5 was phosphorylated *in vitro* by Eg2. The protein was then analyzed by mass spectrometry by Gilles Lajoie and as a result, serine 543 was proposed as a potential Eg2 phosphorylation site. To our opinion, serine 543 was a good candidate because first Eg2 is a Ser/Thr kinase and second it is located in Eg5 stalk, in agreement with Giet *et al* (Giet et al., 1999).

In a first approach, the predicted site was verified by using the same truncated version of Eg5, GST-Eg5(1-634), as used by Giet *et al* (Giet et al., 1999). Therefore, a GST-Eg5 mutant was generated, in which the potential Eg2 phosphorylation site, serine 543 was mutated to alanine, GST-Eg5 S543A.

To test this mutant, phosphorylation experiments were performed. GST-Eg5 S543A was incubated in the presence of Eg2 kinase and radioactive [γ^{32}P]ATP, followed by analysis by SDS-polyacrylamide gel electrophoresis (SDS-PAGE). The autoradiography of the SDS-PAGE gel shows that GST-Eg5 WT is phosphorylated by Eg2 *in vitro*, whereas GST-Eg5 S543A is not (Fig. 8A). This indicates that serine 543 is the Eg2 phosphorylation site of truncated Eg5 *in vitro*.

3.1.1.2 Eg2 phosphorylates full length Eg5 on Serine 543 *in vitro*

A full length Eg5 mutant was generated, in which serine 543 was mutated to alanine,. To test this Eg5 S543A mutant, phosphorylation experiments were carried out *in vitro*. Eg5 S543A was incubated in the presence of Eg2 kinase plus radioactive [γ^{32}P]ATP. Thereafter, the mutant was immunoprecipitated, followed by analysis on SDS-PAGE. To our surprise, in contrast to GST-Eg5 S543A, Eg5 S543A was similarly phosphorylated compared to Eg5 WT, as revealed by the autoradiography (Fig. 1B).

Two hypotheses were proposed to explain these contrasting results: either Eg2 could phosphorylate Eg5 on a second site in Eg5 tail, which was missing in the GST-Eg5 construct, or Eg2 could phosphorylate Eg5 on a second site in the tag, as the two Eg5 constructs also differ in their tag sequences.

As a consequence, we decided to search further for this new Eg2 site by mass spectrometry. After comparison of the mass spectrometry profiles between phosphorylated Eg5 S543A and Eg5 WT, another Eg2 phosphorylation site was revealed by the analysis of Gilles Lajoie. This second Eg2 phosphorylation site was not in the tail but at serine 2. We believed serine 2 to be an artificial Eg2 phosphorylation site. Indeed, serine 2 belongs to a stretch of amino acids with a high probability to be phosphorylated by Eg2 as predicted by Group-based Phosphorylation Scoring (GPS). This stretch of amino acid starts in the Eg5 non-coding linker sequence and ends at the fifth amino acid of Eg5 coding sequence.

The GPS program also confirmed that mutations in the Eg5 linker of arginines -1 and -2 to alanines would prevent phosphorylation. For this reason, the two arginines in Eg5 linker sequence were mutated to alanines, generating Eg5 S543A' and Eg5 WT' for comparison. Phosphorylation experiments were performed to test Eg5 S543A'. After incubation with Eg2 kinase and radioactive [γ^{32}P]ATP, Eg5 S543A' was immunoprecipitated and analyzed by SDS-PAGE. As shown on the autoradiography (Fig. 1C), Eg5 S543A' is not as phosphorylated as Eg5 WT'. This indicates that serine 2 was indeed an artificial phosphorylation site as mutations in Eg5 non-coding sequence prevented Eg2 phosphorylation at this site. Furthermore, this observation suggests that serine 543 is the real phosphorylation site where Eg2 phosphorylates full length Eg5 *in vitro*.

Furthermore, as a control, Eg2 phosphorylation of full length Eg5 and truncated GST-Eg5 were compared. The autoradiography of the phosphorylation experiment (Fig. 1D) shows no striking difference, indicating that they are comparably phosphorylated by Eg2.

Taken together, these results suggest that Eg2 phosphorylates Eg5 on serine 543 *in vitro*.

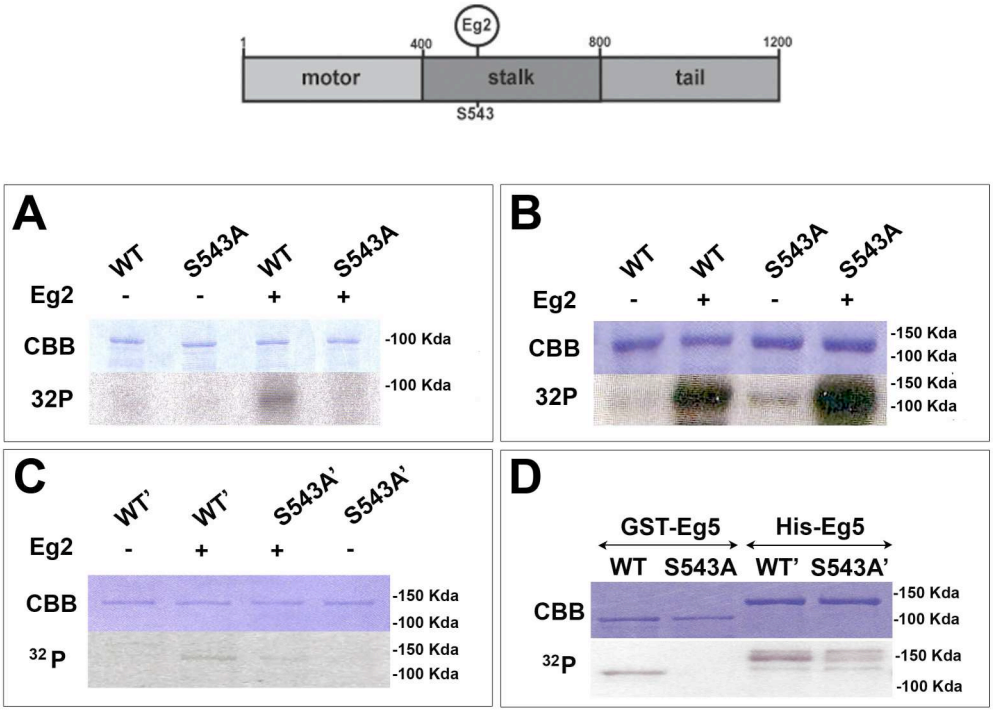

Figure 8: *Xenopus laevis* Eg5 is phosphorylated by Eg2 *in vitro*. CBB, coomassie; ^{32}P, autoradiography, +, kinase added; -, without kinase. (A) *In vitro* phosphorylation of GST-Eg5 by Eg2. WT, GST-Eg5 wild-type; S543A, GST-Eg5 S543A. (B) Eg5 is not phosphorylated by Eg2 *in vitro*. WT, Eg5 wild-type; S543A, Eg5 S543A. (C) Eg5' is phosphorylated by Eg2 *in vitro*. (D) Comparison between GST-Eg5 and Eg5' phosphorylations by Eg2 *in vitro*.

3.1.2 Cdk1 is the major kinase that phosphorylates Eg5 in *Xenopus* egg extract

To continue the study of Eg5 phosphorylation, another Eg5 mutant was generated, in which the known site T937 was mutated to alanine to prevent Eg5 phosphorylation by Cdk1. To verify that T937 is the Eg5 Cdk1 phosphorylation site, Eg5 T937A was immunoprecipitated after *in vitro* incubation with Cdk1 kinase and radioactive [γ^{32}P]ATP followed by SDS-PAGE analysis. The autoradiography of the SDS-PAGE gel (Fig. 2A) reveals that Eg5 T937A is less phosphorylated than Eg5 WT, confirming that T937 is the major phosphorylation site of Eg5 for Cdk1 *in vitro*.

Hence, with the two mutants, Eg5 S543A' and Eg5 T937A, Eg5 phosphorylation in *Xenopus* egg extract could be examined. Both mutants were incubated in mitotic egg extract in the presence of radioactive [γ^{32}P]ATP. The immunoprecipitated proteins were thereafter analyzed by SDS-PAGE. Interestingly, the two mutants gave different results as seen on the autoradiography. Whereas Eg5 S543A' is as phosphorylated as Eg5 WT' (Fig. 9B), the

overall phosphorylation of Eg5 T937 decreases of about 80% when compared to Eg5 WT (Fig. 9B) in mitotic egg extract. These results clearly demonstrate that, in contrast to Eg2, Cdk1 is the major kinase that phosphorylates Eg5 in *Xenopus* egg extract.

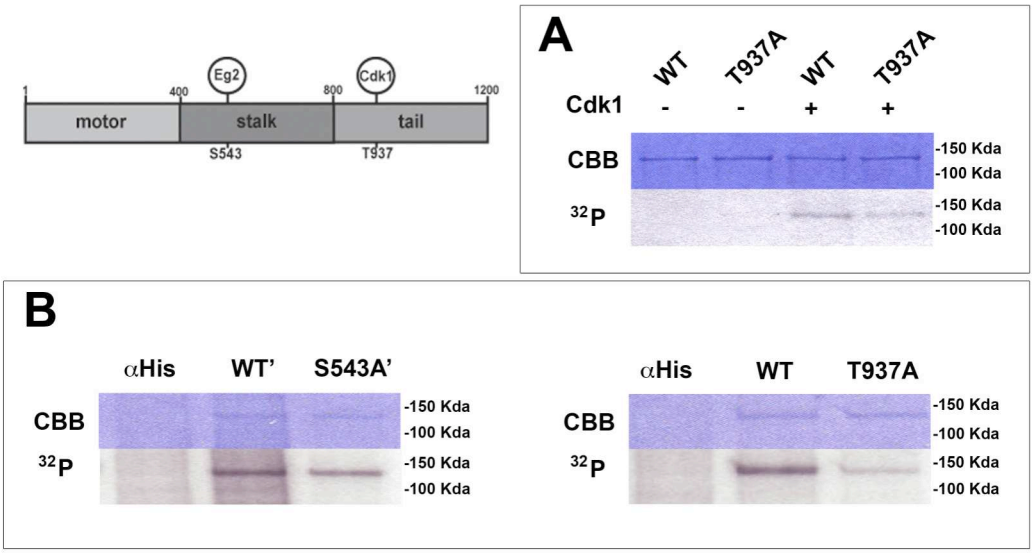

Figure 9: *Xenopus laevis* Eg5 is phosphorylated by Cdk1 *in vitro* and in *Xenopus* egg, but not by Eg2 in *Xenopus* egg extract. (A) *In vitro* phosphorylation of wild-type Eg5 and Eg5 T937A by Cdk1/cyclin B *in vitro*. (B) Phosphorylation of wild-type and mutated Eg5 by Eg2 (left) and Cdk1/cyclin B (right) in mitotic egg extract.

3.1.3 Eg5 S543A' and Eg5 T937A are functional motors *in vitro*

We next wanted to examine whether Eg5 phosphorylation is important for its function during spindle assembly in *Xenopus* egg extract. But, before doing so, we tested if the mutations themselves did not damage Eg5 ability to move along microtubules. Therefore, *in vitro* microtubule gliding assays on glass surfaces were performed. Both mutants were able to bind and move microtubules (Fig. 10A). In addition, microtubule gliding velocities were roughly similar to Eg5 WT with a speed of about 2μm/min (Fig. 10B). These results show that Eg5 S543A' and Eg5 T937A are functional motors.

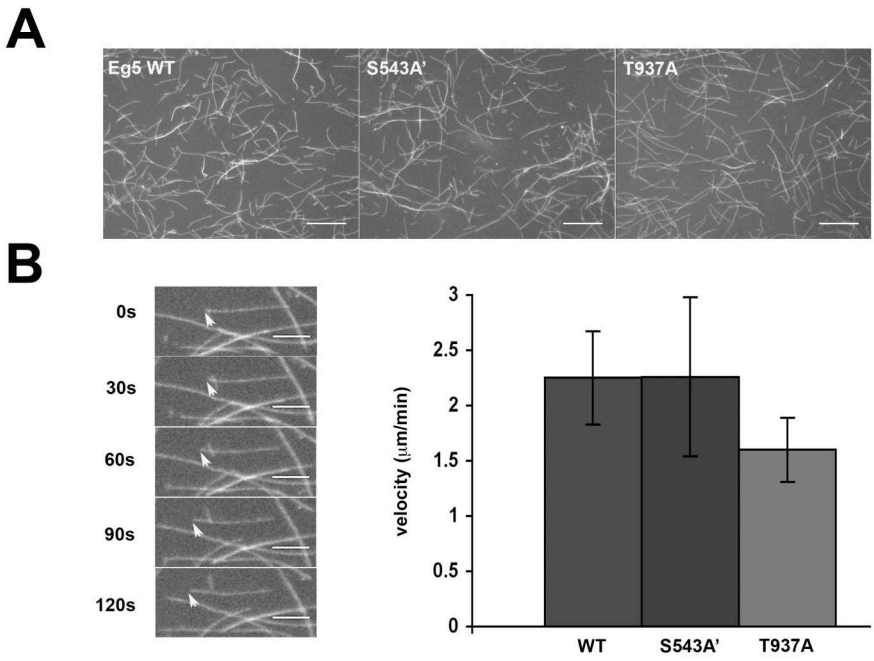

Figure 10: Non-phosphorylatable Eg5 mutants support microtubule gliding *in vitro*. (A) Fluorescence microscopy images of rhodamine-labelled microtubules bound to Eg5 adsorbed to a glass surface. Eg5 (left), Eg5 S543A' (middle) and Eg5 T937A (right) recruit microtubules to the surface with similar efficiency Scale bars are 10μm. (B) Velocity of microtubule gliding. Scale bars are 5μm.

3.1.4 Cdk1 phosphorylation, but not Eg2 phosphorylation is required for spindle assembly in *Xenopus* egg extract

Having confirmed that the mutants were functional motors, we could investigate the role of Eg5 phosphorylation in bipolar spindle formation in *Xenopus* egg extract.

To do so, we performed depletion-add back experiments. We removed the endogenous Eg5 from CSF-extract by immunodepletion and cycled spindles were assembled as described in material and methods (Fig. 11A). As judged by Western blotting, no endogenous Eg5 could be detected after depletion and recombinant proteins were added to a final concentration 400nM, which was reported to be Eg5 endogenous concentration (Fig. 11A). Moreover, observation of the structures formed after 45min incubation revealed that Eg5 depletion severely impaired bipolar spindle formation. Only 20% bipolar spindles could form in Eg5 depleted extract against 85% in control extract. Instead of bipolar spindles, monopolar spindles were predominantly observed in Eg5 depleted extract (Fig. 11B). Remarkably, bipolar spindle assembly was only altered in the presence of Eg5 T937A. Whereas Eg5

S543A' could rescue bipolar spindle formation as well as recombinant Eg5 (Fig. 11B), Eg5 T937A led to the formation of monopolar spindles such as in Eg5 depleted extract (Fig. 11C). No evident changes in spindle morphology, besides a slight decrease in spindle length when compared to Eg5 WT' were observed in the presence of Eg5 S543A'. Our results demonstrate that Cdk1 phosphorylation is essential for Eg5 to function in assembling bipolar spindles in *Xenopus* egg extract, whereas Eg2 phosphorylation is not.

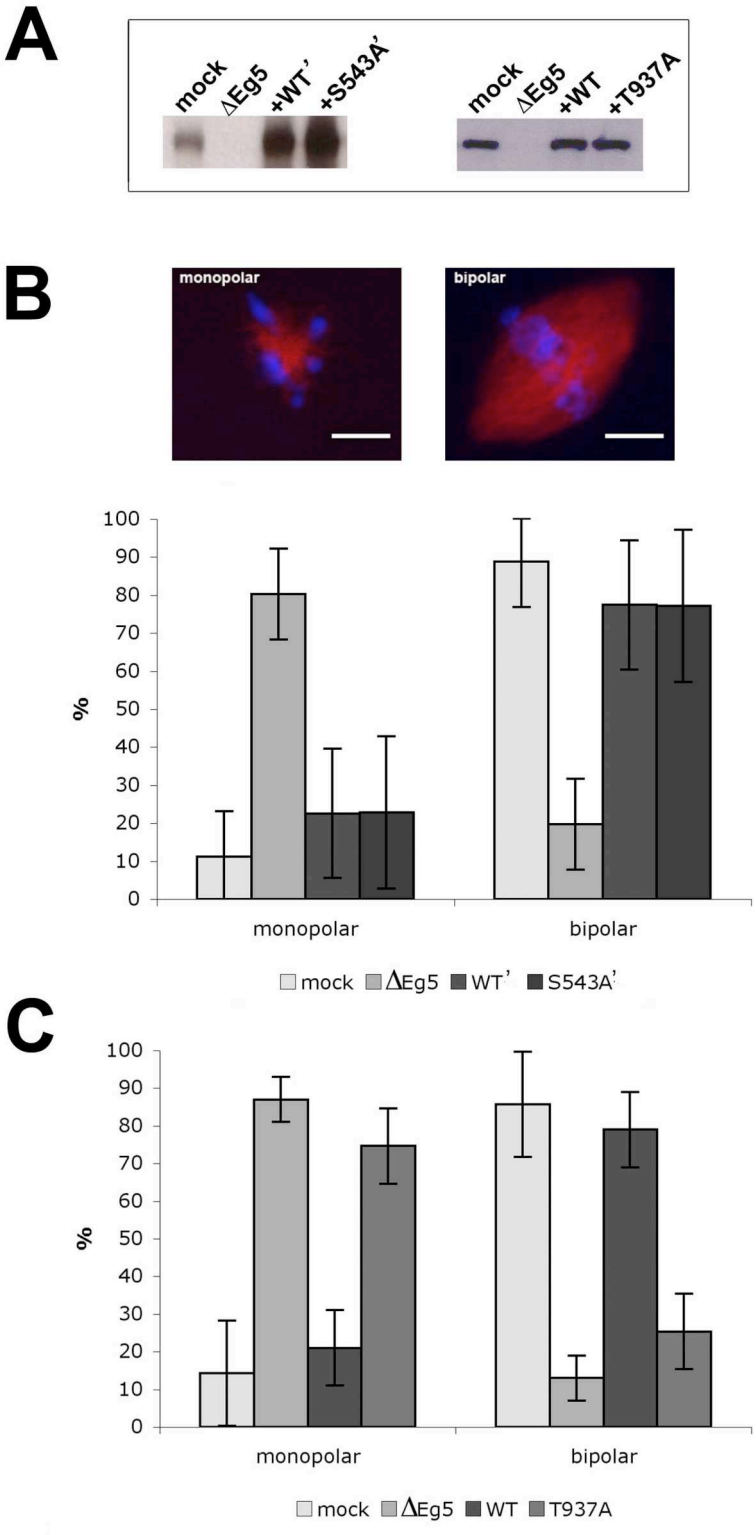

Figure 11: Spindles assemble in Eg5-depleted *Xenopus* egg extract in the presence of Eg5 S543A', but not in the presence of Eg5 T937A. (A) Amounts of Eg5 in *Xenopus* egg extract after 'mock'-depletion (mock), after depletion (ΔEg5) and after addition of recombinant proteins to depleted extract as determined by Western blot. (B) Fluorescence microscopy image of a monopolar spindle and of a bipolar spindle (right). Microtubules are rhodamine-labelled (red) and DNA is stained with Hoechst (blue). Scale bar is 10 μm. Percentage of monopolar and bipolar spindles formed after add back of Eg5 S543A' (C) Percentage of monopolar and bipolar spindles formed after add back of Eg5 T937A.

3.1.5 Eg5 T937A localization to spindle microtubule is disrupted in *Xenopus* egg extract

It has been previously reported that Klp61F, Eg5 *Drosophila* homolog, does not localize to spindle microtubules if not phosphorylated by Cdk1 (Goshima and Vale, 2005). Since we found that Eg5 T937A binds microtubules in microtubule *in vitro* gliding assays, Eg5 T937A localization was further investigated in *Xenopus* egg extract.

In a first approach, the structures obtained after depletion-add back experiments were either immunostained with an anti-Eg5 antibody or pelleted and analyzed for Eg5 presence by western blot. However, the results obtained with these experiments were not consistent.

Therefore, GFP tagged versions of Eg5 WT and Eg5 T937A were used in order to directly follow the protein behavior in extract using confocal microscopy. GFP fusion did not perturb Eg5 function as GFP-Eg5 WT rescued spindle formation after Eg5 depletion in *Xenopus* egg extract. GFP-Eg5 T937A prevents bipolar spindle assembly, similarly to the untagged protein. Moreover, GFP-Eg5 T937A was almost not observed on microtubules of monopolar spindles (Fig. 12A).

Since, it has been reported that a certain amount of Eg5 needs to be present on microtubules to allow spindle formation, the amount of Eg5 T937A and Eg5 WT were quantified. Quantification of the GFP-Eg5 T937A signal over the rhodamine microtubule signal showed that 20 times less GFP-Eg5 T937A localized to microtubules when compared to GFP-Eg5 WT (Fig. 12B). These findings indicate that Cdk1 phosphorylation regulates Eg5 localization to spindle microtubules in *Xenopus* egg extract.

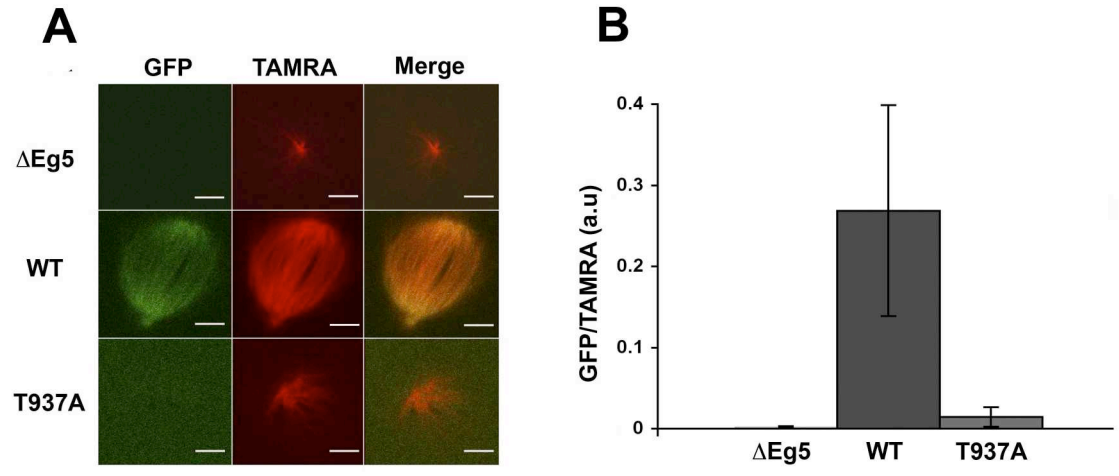

Figure 12: Eg5 T937A does not localize efficiently to microtubules of monopolar spindles in Eg5-depeted egg extract. (A) Confocal fluorescence microscopy images of a monopolar

spindle in Eg5-depleted extract (top), of a bipolar spindle after add back of wild-type Eg5-GFP (left) and of a monopolar spindle after add back of Eg5 T937A-GFP (bottom) to Eg5 depleted extract. Fluorescence of Eg5-GFP (left, green), of rhodamine-labelled microtubules (red, middle) is shown together with merged images (right). Scale bar is 10μm. (B) Average ratio of the fluorescence intensities measured in the GFP channel divided by the fluorescence intensities measured in the rhodamine channel for depleted extract (ΔEg5), for the add back of Eg5-GFP and Eg5 T937A–GFP.

3.2 Role of Eg5 intrinsic motor properties in spindle formation in *Xenopus* egg extract

The depletion-add back experiments suggest that Eg5 needs to be phosphorylated by Cdk1 to interact with spindle microtubules and therefore to function in bipolar spindle assembly in *Xenopus* egg extract. However, they do not explain how bipolar spindle formation occurs when Eg5 is localized to spindle microtubules, or which particular feature of Eg5 is required for bipolar spindle formation. Are Eg5 bipolar organization and cross-linking activity sufficient or are Eg5 motor properties also needed? To tackle this question, we decided on one hand to examine the contribution of Eg5 motor properties to spindle assembly by generating Eg5 chimeras in which Eg5 motor domain has been replaced by other kinesin motor domains and on the other hand to investigate Eg5 motor properties by developing a microtubule gliding assay in *Xenopus* egg extract.

3.2.1 Eg5 chimeras

3.2.1.1 Kid-Eg5, Dkhc-Eg5 support microtubule gliding

To examine the contribution of Eg5 motor properties to spindle assembly, Eg5 chimeras were generated, in which the Eg5 motor domain has been replaced by other kinesin motor domains. Since Eg5 has been characterized as a slow plus-end and mildly processive mitotic motor, the similarly slow plus-end and mildly or non-processive mitotic motor domain of the chromokinesin XKid and on the contrary, the fast plus-end and highly processive non-mitotic motor domain of *Drosophila melanogaster* Kinesin-1 were chosen.

Chimeras, Kid-Eg5 and Dkhc-Eg5, were designed by aligning the different sequences amongst them and by determining the end of the respective neck linker. By doing so, the "motile unit" of Kid and Dkhc, motor domain and neck linker, were preserved. To assess their

motor functionalities, both chimeras were tested by motility assay *in vitro*. Microtubule gliding is observed with both chimeras. Interestingly, the measured speed corresponds to the original speed of the replacing motor domain. Thus Kid-Eg5 moves microtubules with a speed of 2μm/min like Xkid (Fig. 13A) and Dkhc-Eg5 with a speed of 22μm/min, like Kinesin-1 (Fig. 13B). This demonstrates that the intrinsic properties of the chosen motor domains are not altered and drive the chimeras motility *in vitro*.

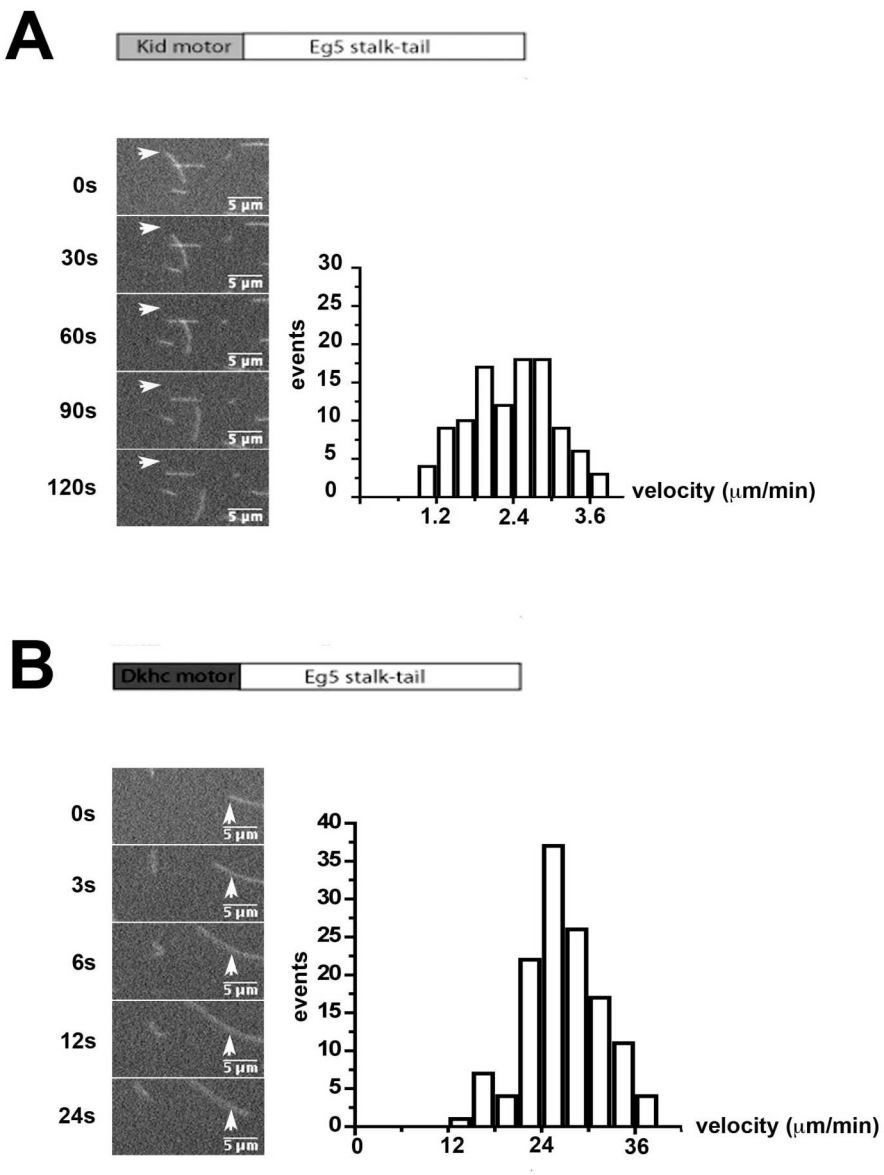

Figure 13: Chimeric Kid-Eg5 and Dkhc-Eg5 mutants support microtubule gliding *in vitro*. (A) Scheme of the chimeric Kid-Eg5 construct (top), and an *in vitro* microtubule gliding assay with Kid-Eg5 as illustrated by fluorescence images of gliding rhodamine-labelled microtubules propelled by Kid-Eg5 at different time points (left) and by a histogram representing the distribution of microtubule velocities (right). (B) Same presentation of microtubule gliding data for Dkhc-Eg5. Scale bars are 5 μm.

3.2.1.2 The specific properties of Eg5 motor domain are required for spindle formation in *Xenopus* egg extract

We next wanted to know if our chimeras could first function in extract and second rescue spindle bipolarity after Eg5 depletion. Therefore, we made a depletion-add back experiment. After removing the endogenous Eg5 from CSF-extract by immunodepletion, cycled spindles were assembled as described in material and methods. The western blot shows that endogenous Eg5 was depleted from the extract and that the two chimeras were added up to the endogenous Eg5 concentration (Fig. 14A).

When the chimeras were added to Eg5 depleted extract, bipolar spindle formation was not rescued and instead new structures were formed (Fig. 14C). This suggests that Kid-Eg5 and Dkhc-Eg5 are both active in mitotic egg extract but unable to substitute for Eg5 activity. Moreover, each chimera gave rise to the formation of different structures, probably as a consequence of their different motor properties.

In the case of Kid-Eg5, the structures observed were short and tight bundles always connected to DNA on one end as well as some monopolar spindles (Fig. 14B). Kid-Eg5 was found preferentially at microtubule plus-ends close to DNA (Fig. 14D). For Dkhc-Eg5, the structures studied were long and thin splayed bundles connected together by DNA. These bundles were loose as they sometimes detached leading to a mixture of single bundles connected to DNA or not (Fig. 14B). In addition, Dkhc-Eg5 was localized all along these bundles (Fig. 14D). The observation that both chimeras are able to bundle microtubules in extract and *in vitro* (data not shown) strongly indicates that they are bipolar motors like Eg5.

Because spindle bipolarity rescue occurs at a certain Eg5 concentration threshold (Goshima et al., 2005), we then tested if bipolarity could be rescued by adding various concentrations of chimeras in add back experiments. For this experiment, Kid-Eg5 chimera was chosen because no bipolar spindle at all were observed in the Dkhc-Eg5 add back experiment (Fig. 14E). Interestingly, the percentage of aberrant structures increases with increasing concentration of Kid-Eg5, while the percentage of Kid-Eg5 induced monopolar spindles decreases. In addition, spindle bipolarity could not be rescued in none of the tested condition. This observation emphasizes that spindle bipolarity requires a unique activity, which is specific of Eg5 motor domain.

All together, these results indicate that Kid-Eg5 and Dkhc-Eg5 are unable to form a bipolar spindle, although they are able to bind spindle microtubules and active in mitotic extract, suggesting that Eg5 intrinsic motor properties are required for bipolar spindle assembly.

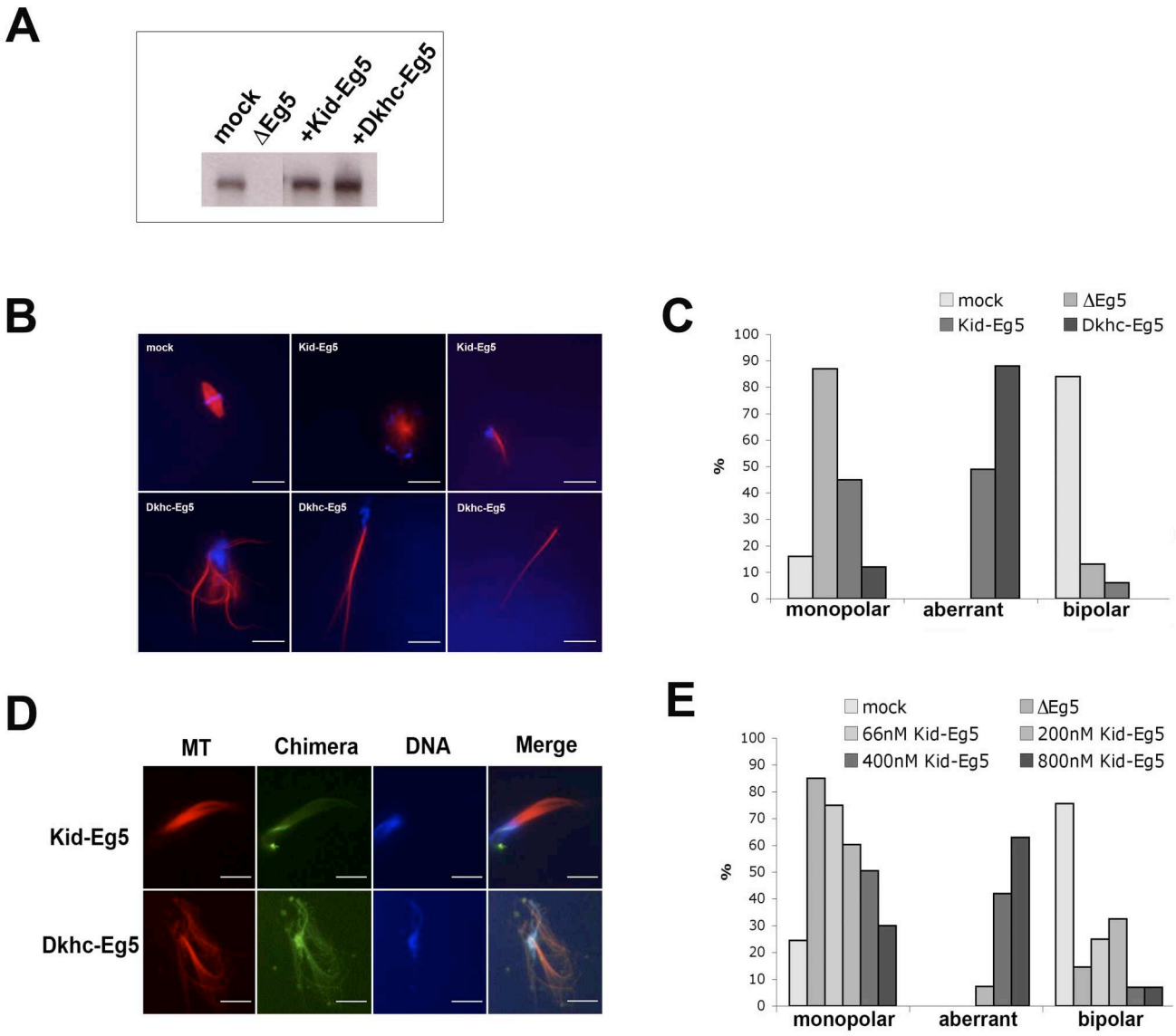

Figure 14: Distinct aberrant spindle phenotypes generated by chimeric Kid-Eg5 and DKhc-Eg5 after addition to Eg5-depleted egg extract. (A) Amounts of Eg5 in *Xenopus* egg extract after 'mock'-depletion (mock), after Eg5-depletion (ΔEg5) and after addition of recombinant proteins to depleted extract (Kid-Eg5, DKhc-Eg5) as determined by Western blot. (B) Fluorescence microscopy images of a bipolar spindle after 'mock'-depletion and of a monopolar spindle and aberrant structures formed after addition of recombinant Kid-Eg5 or DKhc-Eg5 to Eg5 depleted extract. Microtubules are rhodamine-labelled (red) and DNA is stained with Hoechst (blue). Scale bars are 20 μm. (C) Percentage of monopolar, aberrant and bipolar structures formed at the different conditions. (D) Localization of Kid-Eg5 and DKhc-Eg5 in aberrant structures as determined by indirect immunofluorescence (rhodamine-labelled microtubules, red; chimeric motors, green; Hoechst-stained DNA, blue). Scale bars are 10 μm. (E) Percentages of monopolar, aberrant and bipolar structures formed after addition of different concentrations of Kid-Eg5 to Eg5-depleted extract.

3.2.2 Eg5 motility in mitotic *Xenopus* egg extract, development of an assay

3.2.2.1 Microtubule gliding assay in mitotic *Xenopus* egg extract

So far, our study of Eg5 phosphorylation showed that its phosphorylation by Cdk1 is required for its efficient binding to spindle microtubules. In addition to its binding, Eg5 intrinsic motor properties are also essential for Eg5 to function as demonstrated in our study of Eg5 chimeras. To try to get more insight into which of the Eg5 intrinsic properties are needed for bipolar spindle formation, we undertook the development of a microtubule gliding assay in *Xenopus* egg extract.

With such a new assay, Eg5 intrinsic motor properties could be directly investigated in an "*in vivo* like environment", where Eg5 undergoes the same regulatory mechanisms as in a cell. Moreover, *Xenopus* egg extract can be prepared as mitotic or interphasic extracts and is an open system, which allows additional experimental manipulations such as addition or removal of potential regulators.

To develop a microtubule motility assay in extract, we were confronted with two major problems. First, Eg5 needed to be selectively bound onto a surface, while non-specific binding of other microtubule associated proteins (MAPs) and microtubule-dependant motors, present in mitotic extract, had to be prevented. This was achieved by using chemically nano-patterned modified glass surfaces prepared by Jacques Blümmel (Spatz laboratory, University Heidelberg) (Blümmel et al., 2007).

These glass surfaces were first nano-patterned with gold dots to which Eg5 was later adsorbed. The glass surface between nano-dots was then chemically passivated by addition of a layer of polyethylene glycol to prevent binding of proteins from the extract (Fig. 15A).

To test the efficiency of the passivation, flow chambers were assembled using these surfaces. These flow chambers were constructed such that the nano-dots were present only on one side of the chambers, the other side being chemically passivated. Mitotic egg extract was incubated such a flow chamber, followed by microtubule flow. No microtubules were observed to bind onto the surface, suggesting that neither the MAPs, nor the molecular motors present in the extract were recruited to the passivated surface (Fig. 15B).

The ability of the nano-dot attached Eg5 to move microtubules was then tested in an *in vitro* gliding assay on these nano gold dot surfaces. Eg5 was adsorbed on the nano-dots and microtubules were flowed in. The microtubules were able to glide at a velocity of about

2µm/min, which is similar to Eg5 microtubule gliding velocity measured on normal glass surface.

Since Eg5 could be selectively bound to a surface to which none of the MAPs or molecular motors contained in the mitotic extract could attach, the microtubule gliding assay on nano-dots was tested with mitotic *Xenopus* egg extract. In order to do so, Eg5 was adsorbed on the nano-dot surface of a flow chamber, followed by microtubule and mitotic egg extract flows. However, no motility was observed as exogenous microtubules were severed leading to their disappearance within 2 minutes (Fig. 15C). This was not unexpected, as it was previously reported that exogenous microtubules are cut in mitotic egg extract by an enzyme called katanin (McNally and Vale). Therefore, to inhibit katanin activity, anti-katanin antibody was added to the mitotic extract. Microtubule severing activity was reduced but microtubules depolymerized (Fig. 15C). Antibody against XKCM1, which is the major depolymerizing activity in extract, was added in combination with anti-katanin antibody to mitotic extract. In such a treated extract, microtubules were stable enough so that Eg5 driven microtubule gliding could be recorded using fluorescence microscopy (Fig. 15C).

Our results suggest that Eg5 can be selectively bound to a nano-dot patterned surface. Binding of MAPs and molecular motors from the extract is prevented in between the nano-dots and on the other side of the flow chamber by chemically passivating these areas. In addition, exogenous microtubules can be kept stable in mitotic extract for two minutes, allowing microtubule gliding to be recorded.

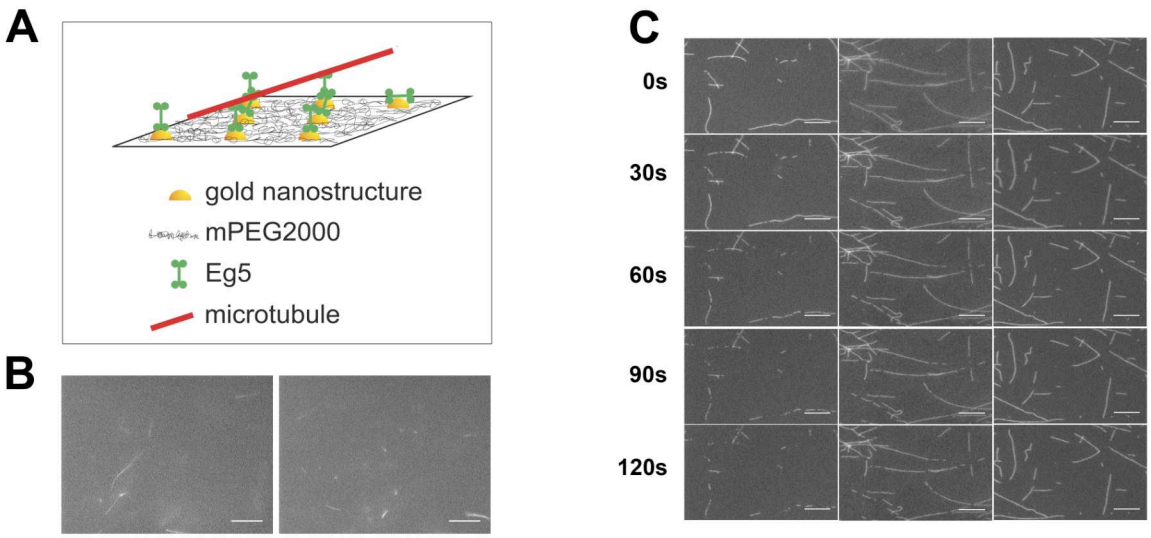

Figure 15: Development of a microtubule gliding assay in mitotic *Xenopus* egg extract.

(A) Scheme of the nano-patterned surfaces. Adapted from (Blümmel et al., 2007). (B) Passivation of the nano-patterned surface against MAPs and molecular motors from mitotic *Xenopus* egg extract. (C) Stabilization of exogenous microtubules in mitotic *Xenopus* egg extract. Left panel: mitotic egg extract; middle panel: mitotic egg extract supplemented with anti-katanin antibody; right panel: mitotic egg extract supplemented with anti-katanin and anti-XKCM1 antibodies. Scale bar is 10μm.

3.2.2.2 Eg5 motility in mitotic *Xenopus* egg extract

Having developed the first microtubule gliding assay in mitotic *Xenopus* egg extract, Eg5 kinetic properties could be assessed in extract. Therefore, Eg5 was adsorbed to the nano-dot surface. Microtubules were flowed in the flow chamber, followed by mitotic extract supplemented with anti-katanin and anti-XKCM1 antibodies. Microtubule velocities were measured in mitotic extract, as well as before extract flow and after extract wash out. Interestingly, Eg5 velocity was on average 40% slower in mitotic egg extract when compared to *in vitro* assays (Fig. 16A-C). Moreover, Eg5 *in vitro* speed recovered after extract removal, showing that the motor was not washed away during the procedure (Fig. 16D).

It has been reported that spindle bipolarity is also ensured by a balance between antagonistic motor activities. To test this hypothesis, we inhibited the major minus-end directed motor, the dynein/dynactin complex and examine whether Eg5 plus-end directed motor properties were altered in a microtubule gliding assay performed in mitotic extract. Therefore, Eg5 was adsorbed to nano-dot surface. Thereafter, microtubules were flowed into the flow chamber, followed by mitotic extract, supplemented with anti-katanin and anti-XKCM1 antibodies. When the dynein/dynactin complex was inhibited by addition of p50, Eg5 driven microtubule gliding velocity almost doubled (Fig. 16B-C).

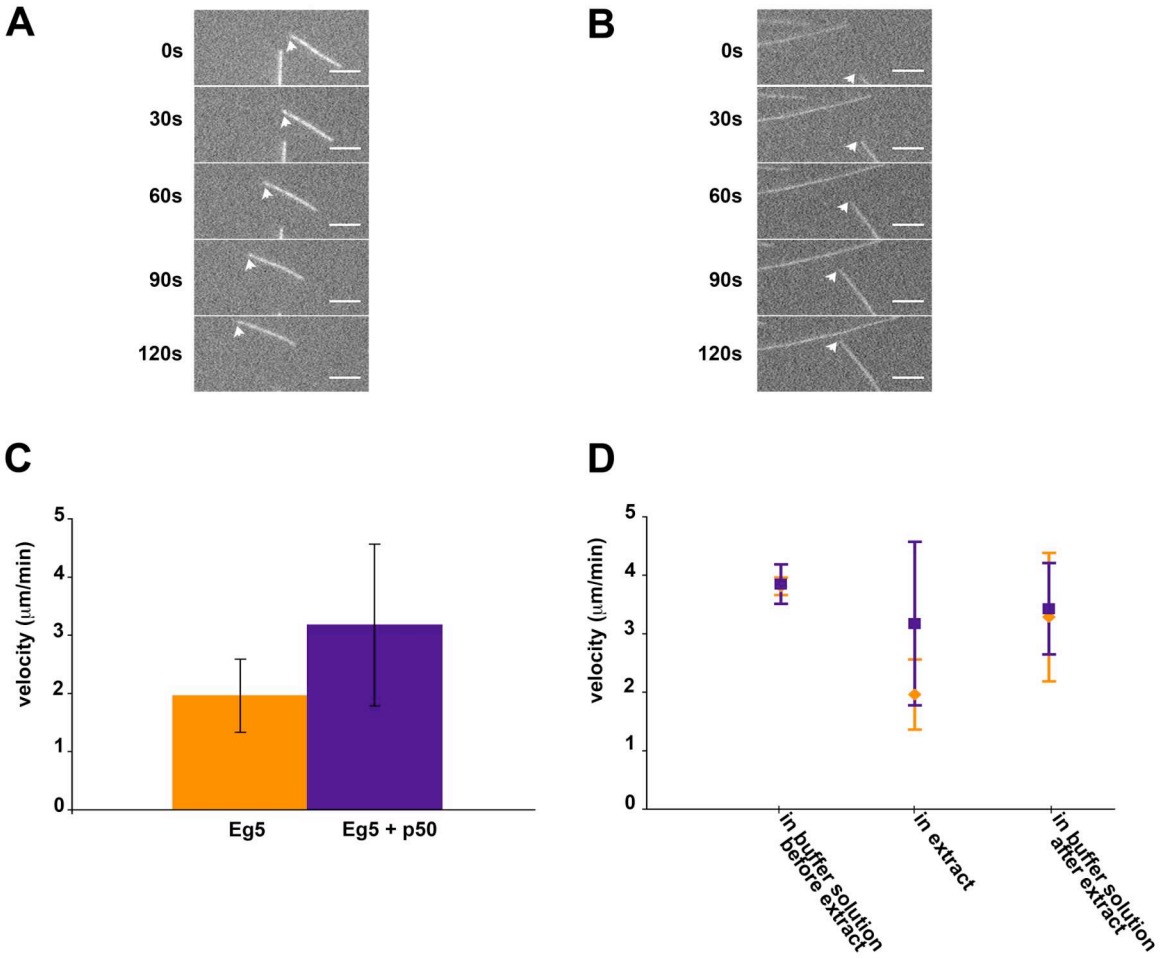

Figure 16: Eg5 driven microtubule gliding assay in mitotic *Xenopus* egg extract.
(A) Eg5 driven microtubule gliding in mitotic *Xenopus* egg extract. (B) Eg5 driven microtubule gliding in mitotic *Xenopus* egg extract in which dynein/dynactin was inhibited. Scale bar is 5µm. (C) Eg5 velocity in mitotic *Xenopus* egg extract. Orange, Eg5 velocity in mitotic *Xenopus* egg extract; purple, Eg5 velocity in mitotic *Xenopus* egg extract in which dynein/dynactin was inhibited. (D) Change in Eg5 velocity between *in vitro* and in mitotic *Xenopus* egg extract.

Our results show that Eg5 velocity decreased in mitotic *Xenopus* egg extract compared to *in vitro* situation. In addition, this decrease cannot be explained by a change in salt concentration. Indeed, salt concentration in extract is supposed to be high and as a consequence Eg5 velocity should increase, which is not the case. Interestingly, Eg5 velocity in mitotic egg extract increases upon dynein/dynactin inhibition, which will be further examined. Furthermore, through this microtubule gliding assay in mitotic egg extract, we provide a new method to study molecular motor regulation.

4 Discussion

4.1 Eg5 phosphorylation by Eg2 is not required for bipolar spindle formation in *Xenopus* egg extract.

Just as it functions in nucleocytoplasmic transport during interphase, RanGTP has been shown to be involved in spindle formation. A RanGTP signaling pathway has already been described and interestingly, one of its key players in spindle formation is Eg2 kinase (Tsai et al., 2003). A previous study has also reported that addition of Eg2 kinase dead mutant (Roghi et al., 1998) leads to the formation of monopolar spindles like those observed when Eg5 has been depleted or inhibited in *Xenopus* egg extract (Sawin et al., 1992a). Moreover, in *Xenopus* egg extract, Eg5 activity is regulated by RanGTP (Wilde et al., 2001). However, how this regulation of RanGTP over Eg5 is molecularly achieved remained unknown. As RanGTP regulates Eg2 kinase activity, which has been shown to phosphorylate Eg5 in its stalk (Giet et al., 1999), we postulated that RanGTP could regulate Eg5 activity through Eg2 phosphorylation of Eg5.

Therefore, we sought to search for Eg2 phosphorylation site in Eg5 entire sequence and actually identified by mass spectrometry serine 543, yet in Eg5 stalk.

Our phosphorylation experiment shows that Eg5 phosphorylation by Eg2 is reduced when S543 has been mutated to alanine, indicating that Eg2 phosphorylates Eg5 *in vitro* at serine 543.

However, Eg2 does not significantly phosphorylate Eg5 in mitotic egg extract. This suggests that Eg2 phosphorylation of Eg5 might not be important in mitotic egg extract.

As a matter of fact, Eg5 S543A' was able to rescue spindle bipolarity as well as recombinant Eg5 in depletion-add back experiments performed in egg extract. This confirms that Eg2 phosphorylation of Eg5, at serine 543 is not important for Eg5 to function in *Xenopus* egg extract. Furthermore, sequence analysis revealed that serine 543 is not conserved among Eg5 homologs, reinforcing the fact that this phosphorylation site is not crucial for Eg5 activity. Nevertheless, Eg2 could still regulate Eg5 by another potentially more indirect mechanism.

4.2 Cdk1 phosphorylation regulates Eg5 efficient binding to spindle microtubule

In contrast to the Eg2 phosphorylation site, Eg5 possesses a Cdk1 consensus phosphorylation site in a conserved sequence among the members of the kinesin-5 subfamily (Heck *et al*, J. Cell. Biol. 1993, 123:665-679). For this reason, Cdk1 phosphorylation of Eg5 has been studied in many different organisms, leading to hypothesize that Cdk1 phosphorylation of Eg5 is required for its interaction with spindle microtubules.

However these studies from various organisms do not clearly demonstrate the link between Eg5 phosphorylation by Cdk1 and loss of spindle bipolarity. Therefore, we addressed Eg5 phosphorylation by Cdk1 in *Xenopus* egg extract, as well as its consequence in spindle assembly in *Xenopus* egg extract.

To do so, the first recombinant Eg5 mutant, where T937 was mutated to alanine in order to prevent Cdk1 phosphorylation, was produced. After having confirmed *in vitro* that T937 is the Cdk1 phosphorylation site of Eg5, Eg5 T937A phosphorylation was examined in mitotic egg extract. In contrast to previous study in HeLa cells reporting that only 20% of total Eg5 phosphorylation can be accounted to Cdk1 (Blangy et al., 1995), we found that Cdk1 is the major kinase that phosphorylates Eg5, as phosphorylation of Eg5 T937 decreased of about 80% when compared to Eg5 WT in mitotic extract.

Eg5 is involved in bipolar spindles formation as its loss or inhibition leads to the formation of monopolar spindles (Mayer et al., 1999) (Sawin et al., 1992a). Interestingly, these monopolar spindles are reminiscent of the structures that were observed after replacement of endogenous Eg5 by Eg5 T937A. Such monopolar spindles were also described to form in *Drosophila* S2 cells transfected with the mutant Klp61F T933A (Goshima and Vale, 2005), leading to the proposal that Klp61F interacts with microtubules Because it was proposed that Cdk1 phosphorylation of Eg5 is important for its interaction with spindle microtubules, Eg5 T937A was quantified on the monopolar structures. Our result shows that Eg5 T937A does not strongly localize to microtubule of monopolar spindles, suggesting that Eg5 phosphorylation by Cdk1 is necessary for Eg5 to efficiently bind spindle microtubules.

Moreover, our findings are in agreement with a previous study demonstrating that the transition from monopolar to bipolar spindles was dependent on the amount of Eg5 present on spindle microtubules (Goshima et al., 2005).

However, although our results in extract clearly show that Eg5 T937 interaction with microtubules is perturbed, our *in vitro* motility assays do not show any. Indeed, Eg5 T937A is

able to bind microtubules (even in high salt buffer) just as Eg5 WT does. And furthermore, Eg5 T937A is a functional motor as microtubule gliding was observed.

There are two major differences between these two assays that could explain this divergence between the results. First, whereas Eg5 is free to diffuse in an add back experiment, it is physically bound to a glass surface, probably in high concentration, in a motility assay, which could lead to favor its interaction with microtubules. Moreover, microtubule organization also differs. In a monoaster, microtubules are mostly arranged in parallel bundles, whereas single microtubules are observed in a gliding experiment. Binding of the Eg5 to parallel microtubule bundles on one hand or to single microtubules on the other hand could also differ.

Cdk1 phosphorylation is essential for Eg5 to interact efficiently with microtubules and hence to function in bipolar spindle assembly. Remarkably, the results also suggest that the mechanism by which Cdk1 regulates Eg5 is conserved in eukaryotes, with the exception of the fission yeast (Goshima and Vale, 2005) (Drummond and Hagan, 1998).

4.3 Eg5 intrinsic motor properties are required for spindle assembly in *Xenopus* egg extract

Our study of Eg5 regulation taught us that Cdk1 phosphorylation is essential for Eg5 to be targeted to microtubules but we do not learn about how Eg5 functions once on spindle microtubule. From previous studies, we know that an active Eg5 motor domain is required for bipolar spindle assembly (Mayer et al., 1999). However, we do not know if all or only some of its intrinsic motor properties are required for spindle formation.

To undertake this question, Eg5 chimeras were generated, in which the Eg5 motor domain was replaced by the motor domains of Xkid and Dkhc, which have distinct motor properties. *In vitro* motility assays show that the chimeras move microtubules with the same speed as the protein from which the motor domain originate from, suggesting that the motility properties were conserved.

Moreover, both chimeras were not only active *in vitro* but also in mitotic *Xenopus* egg extract, as they gave rise to two distinct phenotypes after depletion-add back experiments. This is interesting regarding the fact that Dkhc-Eg5 motor domain comes from kinesin 1, which is not a mitotic motor.

Furthermore, whereas Kid-Eg5 add back leads to the formation of small bundles connected to DNA, long and splayed bundles were observed when Dkhc-Eg5 was added back. This difference in bundle length could be explained by the different motor properties. As Dkhc-

Eg5 is a highly processive, it could sustain microtubule contact for longer time, while its high speed would increase the displacement between microtubules.

Since none of the active chimeras could rescue spindle bipolarity, this indicates that Eg5 intrinsic properties are essential for spindle formation. Eg5 is a bipolar motor, which is able to bundle antiparallel and parallel microtubules. The fact that two chimeras are able to form bundles strongly suggests that they are also bipolar motors. Moreover, the plus-end directed motor Kid-Eg5 is preferentially found next to DNA indicating that Kid-Eg5 bundles are likely to be composed of parallel microtubule arrays. Taken together, this suggests that Eg5 cross-linking activity of parallel microtubules is probably not essential for bipolarity establishment.

In addition, the loss of bipolarity was robust over a wide range of Kid-Eg5 concentration, suggesting that Eg5 motor activity could not be compensated.

Furthermore, although having the same tail domain, the two chimeras are performing different functions. This is interesting in regard to the kinesin phylogenetic tree. The kinesin phylogenetic tree was built according to the sequence homology between the different kinesin motor domains, leading to 14 kinesin related protein (KRP) subfamilies. KRP motor domains, which contain the microtubule and the nucleotide binding sites, share roughly 30% homology. Interestingly, this classification has also yielded to classify KRPs according to their function. This was unexpected as KRP tail, which differs from one KRP to another one, was the only part believed to encode some "functional activity". Our experiments give for the first experimental evidence that KRP motor domain does indeed encode some "functional activity", supporting the phylogenetic classification of KRPs.

4.4 Eg5 motility in *Xenopus* egg extract

So far, our results suggest that not only Cdk1 phosphorylation of Eg5 is required for bipolar spindle formation but also its intrinsic motor properties. Therefore, we sought to investigate Eg5 motor properties, and in particular Eg5 kinetic, in *Xenopus* egg extract. To do so, we developed a microtubule gliding assay in *Xenopus* egg extract.

To date, this assay is the only one that allows the study of molecular motors, and conventional MAPs, in an "*in vivo* like environment", such as *Xenopus* egg extract. Indeed, this assay is performed in egg extract, where proteins are subjected to the same regulatory events as they undergo in cells. However, in contrast to cells, egg extract is an open system, which gives the opportunity to examine protein behavior at a molecular level, by removing or inhibiting potential regulators for example.

As a matter of fact, Eg5 velocity measured in mitotic extract differs from velocity measured *in vitro*. Different parameters can actually influence Eg5 velocity in an extract microtubule gliding assay.

The first, the environment, in which the two gliding assays are performed, differs. This environment can vary for instance in term of salt concentration. *In vitro* gliding assays are performed in buffer solution, which composition can be optimized depending of the protein of interest. In an extract gliding experiment, the environment composition is thought to be suitable for any proteins as it is their "natural environment". As a consequence, *in vitro* microtubule gliding assay were performed in buffer solution in which the salt concentration was elevated to be as close as possible to that of the extract. The results show that Eg5 driven microtubule gliding velocity increased with the salt concentration. Therefore, this difference in salt concentration cannot explain the difference in Eg5 speeds between *in vitro* and in extract experiments.

The second parameter that could infer for a reduced Eg5 speed is a crowed microtubule. In extract gliding assay, MAPs from the extract also bind to microtubules, which reduces the number of binding sites available for Eg5 stepping. This could lead to a decrease of Eg5 velocity as Eg5 is a processive motor. As a matter of fact, Eg5 velocity increases upon dynein/dynactin inhibition, which could be explained if dynein/dynactin indeed challenges Eg5 for microtubule binding.

On the other hand, the minus-end directed dynein/dynactin complex could also compete with Eg5 plus-end directed motility, leading to a decrease in Eg5 speed. In this way, it has been reported that dynactin can associate in a phosphorylation dependant manner with Eg5 (Blangy et al., 1997). Therefore, dynein/dynactin could bind microtubule by binding to some of the Eg5 adsorbed on the nano-dots, hence counteracting Eg5 motility. Besides dynein/dynactin, Eg5 motor properties could also be regulated by other proteins in extract, consequently reducing Eg5 speed.

These interesting findings will definitely be further investigated.

5 Material and methods

5.1 Cloning

5.1.1 Full length Eg5 constructs

Eg5 plasmid was inserted in pFastBac HTa vector (Invitrogen) via a Stu1 restriction site at the 5' and a Not1 at the 3'so that the protein was His tagged at its N terminus. Single point mutations, S543A and T937A, were introduced using Quickchange 2 XL from Stratagene giving rise to two constructs Eg5 S543A and Eg5 T937A.

To abolish residual artificial phosphorylation signal, two additional point mutations in the linker region were done for Eg5 S543A. -R35 and -R36, located in the N terminal tag of the pFastBac vector between the TEV cleavage site and the beginning of Eg5 sequence, were mutated to glycines, generating Eg5 S543A'. For comparison, -R35G and-R36G were also mutated in Eg5 WT, producing Eg5 WT'.

GFP-Eg5 fusion constructs were obtained as described in Uteng *et al* (manuscript in preparation).

5.1.2 Chimeric Eg5 constructs

Kid(1-369)-Eg5(369-1103) was constructed as follows. Kid motor domain was amplified by PCR using 5'GCTGCCATGGTTCTTACTGGGCCTCTC 3' as 5'primer and 5'GGTGGTTTCCTGGCTGAAAG-3' as 3'primer. Thus Nco1 site was introduced at the 5'end, whereas a blunt end was generated at the 3'end. Eg5 sequence was amplified by PCR using 5'ACAAAGAAGGCACTCATCAAGGAG3' as 5' primer and 5'TTCGAAAGCGGCCGCTC3' as 3'primer respectively. This generated a blunt end at the 5'end, while a Not1 site was introduced at the 3'end. The PCR product were digested, phosphorylated and ligated into pFastBac Hta.

The same cloning strategy was used to generate Dkhc(1-354)-Eg5(369-1103).

The primers used for Dkhc-Eg5 are 5'GCTGCCATGGCAATGTCCGCGGAACGAGAG3' for the 5'primer, generating a Nco1 site restriction site and 5'AAGCTCCTCGTTAACGCAG3' for the 3'primer, generating a blunt end. Same Eg5 primers were used.

5.2 Proteins expression and purification

5.2.1 Expression and purification of Eg5 constructs

Full length Eg5 was expressed in Sf9 insect cells and purified as followed. Cells were lysed in lysis buffer (50mM KH_2PO_4, 250mM KCl, 10mM imidazole, 0.5mM MgATP, 0.1% Triton X100, 10mM β-mercaptoethanol, protease inhibitors (Roche), pH8) and centrifuged at 176000g for 30min at 4°C. Supernatant was incubated with Talon resin (Clontech) for 1h at 4°C. Resin was washed with washing buffer (50mM KH_2PO_4, 250mM KCl, 10mM imidazole, 0.1mM MgATP, 10% glycerol, protease inhibitors (Roche),10mM β-mercaptoethanol pH8) and protein was eluted with elution buffer (50mM KH_2PO_4, 150mM KCl, 250mM imidazole, 0.1mM MgATP, 10% glycerol, protease inhibitors (Roche), pH7). The protein was dialysed overnight in dialysis buffer (50mM KCl, 50mM imidazole, 0.5mM EGTA, 10% sucrose, 10mM β-mercaptoethanol, pH 7) at 4°C. If the protein was used for add back experiment, the β-mercaptoethanol free dialysis buffer was degazed and dialysis lasted for 3h. Finally, the protein was aliquoted in maximum 10ul aliquot, frozen in ethane and stored in liquid nitrogen.

Eg5 T937A, Eg5 S543A', Kid-Eg5, Dkhc-Eg5, GFP-Eg5 T937A were expressed and purified following the same protocol as Eg5. GFP-Eg5 WT was expressed and purified as described in Uteng *et al* (manuscript in preparation).

5.2.2 Expression and purification of Eg2

BL21-RIL *E. coli* were transformed with pET28a-Eg2 (gift from Teresa Sardon). Expression was induced with 0.3mM IPTG and cells were harvested after 4h expression at 30°C. Pelleted cells were lysed in lysis buffer (25mM HEPES, 330mM KCl, 5mM $MgCl_2$, 0.1% TritonX100, 5mM β-mercaptoethanol, protease inhibitors (Roche), pH7). Then, Eg2 was purified over a Talon resin (Clontech) and eluted with elution buffer (25mM HEPES 330mM KCl, 5mM $MgCl_2$, 10% glycerol, 300mM imidazole, 5mM β-mercaptoethanol, protease inhibitors, pH7.5). Eg2 was dialyzed overnight at 4°C in dialysis buffer (25mM HEPES, 250mM KCl, 2mM $MgCl_2$, 10% glycerol, 1mM DTT, pH 7.5), aliquoted, frozen in liquid nitrogen and stored at -80°C.

5.2.3 Expression and purification of p50

Expression and purification were performed according to (Wittmann and Hyman, 1999).

5.2.4 Antibody purification

5.2.4.1 Eg5 antibody

GST-Eg5, purified as described in Sawin *et al* (Nature 1992, 359:540-543) was injected into rabbits (Eurogentec). Eg5 was coupled to NHS-activated HiTrap column (Amersham) according to the manufacture instructions. For affinity purification, the serum was recirculated over the column overnight at 4°C. The column was washed with washing buffer (0.5M NaCl, 0.1% Triton X100, Phosphate-buffered saline, PBS) followed by elution with 0.1M glycine pH2.6 in Eppendorf tubes containing 10% (v/v) of 2M Tris pH8. The antibody was dialysed overnight in PBS/50% glycerol and stored at -20°C.

5.2.4.2 XKCM1 antibody

The α-XKCM1 antibody was purified as described in (Walczak et al., 1996).

5.2.4.3 Katanin antibody

The α-Katanin antibody was purified as described in (McNally and Thomas, 1998).

5.3 Phosphorylation experiments

In vitro phosphorylation of Eg5 was performed by incubating 1μg of Eg5 in 20μl with either 0.1μg of Cdk1/cyclinB (Cell Signaling) or 0.2μg of Eg2. Phosphorylation reactions were carried out for 30min at room temperature in CSF-XB (100mM KCl, 0.1mM $CaCl_2$, 3mM $MgCl_2$, 10mM HEPES, 50mM sucrose, 5mM EGTA, pH7.7) containing 10μM MgATP and 0.75μCi/μl radioactive [γ^{32}P]ATP (Amersham). After 2h incubation on ice, Eg5 was immunoprecipitated using anti-His antibody (Qiagen) coupled to proteinG dynabeads from the phosphorylation reaction, which was diluted with 20μl CSF-XB + phosphatase inhibitors (100mM NaF, 80mM Glycerophosphate, 1mM PMSF, 20mM EDTA, 1mM sodium vanadate, 1μM microcysteine and protease inhibitors (Roche)).

Beads were retrieved, boiled and loaded on a 10% SDS-PAGE gel. The gel was exposed to a Kodak Biomax film.

The same protocol was followed for phosphorylation experiments in mitotic egg extract, except that phosphorylation reactions were performed in *Xenopus* mitotic egg extract with a final radioactive [γ^{32}P]ATP concentration of 15μCi/μl.

5.4 *Xenopus* egg extract experiment

5.4.1 Preparation of *Xenopus* egg extract

Cytostatic factor arrested extracts (CSF extract) were prepared as described by Murray (Murray A.W, Methods Cell. Biol. 1991, 36:581-605) except that eggs were packed 1min at 600g then1min at 1200g and crushed at 10000g, 18min, 16°C, acceleration slow. Spindle assembly was performed as described in Peset *et al* (J. Cell. Biol. 2005, 170:1057-1066). Briefly, TAMRA labeled tubulin (Hyman *et al*, Methods Enzymol 1991, 196:478-485) and sperm nuclei were added to CSF extract, half of which was sent was to interphase with calcium solution (0.4mM $CaCl_2$, 10mM KCl, 0.1mM $MgCl_2$), while the other half was kept on ice. After usually 60min, interphasic nuclei were observed and the extract was cycled back to mitosis with the addition of the other half of CSF extract.

5.4.2 Depletion-add back experiments

80μl of anti-Eg5 antibody coupled proteinA dynabeads were used to deplete 100μl extract for 1h on ice. Spindle assembly was performed as described above. Recombinant proteins or buffer as a control were added with depleted CSF extract as the reaction was cycled back to mitosis. After 45min extracts were diluted with dilution buffer (30% glycerol, 0.5% Triton X100 in BRB80 (80 mM PIPES, 1mM $MgCl_2$, 1mM EGTA, pH 6.8)), fixed with fixation buffer (dilution buffer with 4% formaldehyde) and layered on top of a 3ml cushion (30% glycerol in BRB80). After centrifugation at 3000rpm, 30min, 20°C (Hereaus centrifuge), cover slips were post-fixed in methanol at -20°C. After rehydratation in PBS/0.1% Triton X100, coverslips were incubated with anti-Eg5 antibody, washed and incubated with alexa488 anti rabbit antibody (Molecular Probes). Hoechst (H33342, Sigma) was used to stain DNA. Then coverslips were washed and mounted. Depletion efficiency was assayed by Western Blot. Images were taken using an inverted microscope (Axiovert 135TV, Zeiss, 100W

mercury, CDD camera, Coolsnap Photometric) with an oil immersion 63X objective (Zeiss). Structures were quantified from at least 3 different experiments.

For GFP-Eg5 localization, images were taken from non-fixed samples with confocal microscope (Zeiss LSM 510 Meta) with a 63X water immersion objective (Leica). For quantification, a region of interest was drawn in which the mean intensity per area was measured using ImageJ. After background subtraction, ratios of GFP intensities over TAMRA intensities were calculated and averaged over 10 structures.

5.5 Microtubule gliding assay

5.5.1 *In vitro* microtubule gliding assay

Tetramethylrhodamine (TAMRA, Molecular Probes) labeled microtubules were generated by polymerizing 5μg/μl tubulin (Castoldi and Popov, 2003) with 0.1μg/μl TAMRA tubulin, 1mM guanosine 5'-triphosphate, GTP, in BRB80.

After a tenfold dilution in BRB80 containing 20μM taxol (paclitaxel, Sigma), microtubules were pelleted 10min in a tabletop centrifuge at 140000rpm (Eppendorf 5417C). For use, microtubule pellet was resuspended and further diluted 1:1000 in BRB80/taxol.

A flow chamber was built by assembling 2 cleaned ethanol coverslips on top of each other using double sticky tape. Flow chamber volume was about 5μl.

One flow chamber volume of BRB80 was first flowed in, followed by the motor mix (3μM motor protein and 10mM MgATP). After 5min incubation on ice, one flow cell of washing buffer (10mg/ml BSA, 10mM MgATP in BRB80) was introduced and followed by another 5min incubation. Microtubules mix (10mg/ml BSA, 10mM MgATP, 0.25mg/ml glucose oxidase, 0.12mg/ml catalase, 25mM glucose, microtubules 1:5, in BRB80) was flowed in at room temperature.

To image, an inverted microscope (as described above) was used. Usually sequences of 2min time lapse were recorded with 1 frame taken every 10s and 100ms exposure time per frame. Velocities were analyzed by kymographs by using a macro developed by Arne Seitz on ImageJ (Seitz and Surrey, 2006). One kymograph was constructed per microtubule and 10 to 20 microtubules were analyzed per time lapse series. Average microtubule velocity per time lapse series was obtained by a Gauss fit. Three time-lapse series were recorded per flow chamber, each flow chamber repeated twice from which the arithmetic average was calculated.

5.5.2 In extract microtubule gliding assay

Gold dots surfaces were done as described in (Blümmel et al., 2007).

A flow chamber of about 5-10ul was built by putting the cover slip with the nanostructures on top of a cover slip, which surface has been passivated. The 2 cover slips were assembled via 2 layers of double sticky tape. Microtubules were prepared as described above.

One flow chamber volume of Eg5 dialysis buffer containing 10mM ATP was introduced. The motor protein ([Eg5]=700nM, 10mM ATP in Eg5 dialysis buffer) was then flowed in and the flow chamber was incubated for 10 min on ice. The flow chamber was washed with 5 volumes of Eg5 dialysis buffer containing 10mM ATP. Microtubule solution (10mM ATP, 0.25mg/ml glucose oxidase, 0.12mg/ml catalase, 25mM glucose, microtubule 1:5, in Eg5 dialysis buffer/20µM taxol) was introduced, followed by 5min incubation at room temperature. Unbound microtubules were washed with one volume of microtubule solution without microtubules.

The flow chamber was brought to the microscope (as described above) where a first movie was recorded. Then 3 volumes of freshly thawed mitotic extract were flowed in. The extract was previously incubated 1h on ice with 50µg/µl anti-katanin, 90µg/µl anti-XKCM1, 10µM RanQ69L, 20µM nocodazole and 0.9mg/ml of p50 if added. After recording of movies in extract, the flow chamber was washed with 3 volumes of Eg5 dialysis buffer containing 10mM ATP and one volume of microtubule solution was introduced. After 5min incubation and washing of unbound microtubules, movies were recorded as described above.

6 References

Blangy, A., Arnaud, L., and Nigg, E. A. (1997). Phosphorylation by p34cdc2 protein kinase regulates binding of the kinesin-related motor HsEg5 to the dynactin subunit p150. J Biol Chem *272*, 19418-19424.

Blangy, A., Lane, H. A., d'Herin, P., Harper, M., Kress, M., and Nigg, E. A. (1995). Phosphorylation by p34cdc2 regulates spindle association of human Eg5, a kinesin-related motor essential for bipolar spindle formation in vivo. Cell *83*, 1159-1169.

Blümmel, J., Cahu, J., Sandblad, L., Schmitz, C., Surrey, T., and Spatz, J. (2007). Motor Protein Driven Microtubule Transport on Gold Particle Nanopattern, Submitted edn: Submitted).

Brady, S. T. (1985). A novel brain ATPase with properties expected for the fast axonal transport motor. Nature *317*, 73-75.

Cameron, L. A., Yang, G., Cimini, D., Canman, J. C., Kisurina-Evgenieva, O., Khodjakov, A., Danuser, G., and Salmon, E. D. (2006). Kinesin 5-independent poleward flux of kinetochore microtubules in PtK1 cells. J Cell Biol *173*, 173-179.

Carazo-Salas, R. E., Gruss, O. J., Mattaj, I. W., and Karsenti, E. (2001). Ran-GTP coordinates regulation of microtubule nucleation and dynamics during mitotic-spindle assembly. Nat Cell Biol *3*, 228-234.

Castoldi, M., and Popov, A. V. (2003). Purification of brain tubulin through two cycles of polymerization-depolymerization in a high-molarity buffer. Protein Expr Purif *32*, 83-88.

Caudron, M., Bunt, G., Bastiaens, P., and Karsenti, E. (2005). Spatial coordination of spindle assembly by chromosome-mediated signaling gradients. Science *309*, 1373-1376.

Crevel, I. M., Alonso, M. C., and Cross, R. A. (2004). Monastrol stabilises an attached low-friction mode of Eg5. Curr Biol *14*, R411-412.

Dagenbach, E. M., and Endow, S. A. (2004). A new kinesin tree. J Cell Sci *117*, 3-7.

Desai, A., and Mitchison, T. J. (1997). Microtubule polymerization dynamics. Annu Rev Cell Dev Biol *13*, 83-117.

Drummond, D. R., and Hagan, I. M. (1998). Mutations in the bimC box of Cut7 indicate divergence of regulation within the bimC family of kinesin related proteins. J Cell Sci *111 (Pt 7)*, 853-865.

Ems-McClung, S. C., Zheng, Y., and Walczak, C. E. (2004). Importin alpha/beta and Ran-GTP regulate XCTK2 microtubule binding through a bipartite nuclear localization signal. Mol Biol Cell *15*, 46-57.

Endow, S. A., and Barker, D. S. (2003). Processive and nonprocessive models of kinesin movement. Annu Rev Physiol *65*, 161-175.

Enos, A. P., and Morris, N. R. (1990). Mutation of a gene that encodes a kinesin-like protein blocks nuclear division in A. nidulans. Cell *60*, 1019-1027.

Gibbons, I. R. (1965a). Chemical dissection of cilia. Arch Biol (Liege) *76*, 317-352.

Gibbons, I. R. (1965b). Reactivation of Glycerinated Cilia from Tetrahymena Pyriformis. J Cell Biol *25*, 400-402.

Giet, R., and Prigent, C. (2000). The Xenopus laevis aurora/Ip11p-related kinase pEg2 participates in the stability of the bipolar mitotic spindle. Exp Cell Res *258*, 145-151.

Giet, R., Uzbekov, R., Cubizolles, F., Le Guellec, K., and Prigent, C. (1999). The Xenopus laevis aurora-related protein kinase pEg2 associates with and phosphorylates the kinesin-related protein XlEg5. J Biol Chem *274*, 15005-15013.

Glover, D. M., Leibowitz, M. H., McLean, D. A., and Parry, H. (1995). Mutations in aurora prevent centrosome separation leading to the formation of monopolar spindles. Cell *81*, 95-105.
Goshima, G., and Vale, R. D. (2005). Cell cycle-dependent dynamics and regulation of mitotic kinesins in Drosophila S2 cells. Mol Biol Cell *16*, 3896-3907.
Goshima, G., Wollman, R., Stuurman, N., Scholey, J. M., and Vale, R. D. (2005). Length control of the metaphase spindle. Curr Biol *15*, 1979-1988.
Guse, A., Mishima, M., and Glotzer, M. (2005). Phosphorylation of ZEN-4/MKLP1 by aurora B regulates completion of cytokinesis. Curr Biol *15*, 778-786.
Hagan, I., and Yanagida, M. (1990). Novel potential mitotic motor protein encoded by the fission yeast cut7+ gene. Nature *347*, 563-566.
Heald, R., Tournebize, R., Blank, T., Sandaltzopoulos, R., Becker, P., Hyman, A., and Karsenti, E. (1996). Self-organization of microtubules into bipolar spindles around artificial chromosomes in Xenopus egg extracts. Nature *382*, 420-425.
Heck, M. M., Pereira, A., Pesavento, P., Yannoni, Y., Spradling, A. C., and Goldstein, L. S. (1993). The kinesin-like protein KLP61F is essential for mitosis in Drosophila. J Cell Biol *123*, 665-679.
Hirokawa, N. (1998). Kinesin and dynein superfamily proteins and the mechanism of organelle transport. Science *279*, 519-526.
Hook, P., and Vallee, R. B. (2006). The dynein family at a glance. J Cell Sci *119*, 4369-4371.
Houliston, E., Le Guellec, R., Kress, M., Philippe, M., and Le Guellec, K. (1994). The kinesin-related protein Eg5 associates with both interphase and spindle microtubules during Xenopus early development. Dev Biol *164*, 147-159.
Howard, J. (2001). Mechanics of motor proteins and the cytoskeleton: Sinauer).
Hoyt, M. A., He, L., Loo, K. K., and Saunders, W. S. (1992). Two Saccharomyces cerevisiae kinesin-related gene products required for mitotic spindle assembly. J Cell Biol *118*, 109-120.
Kalab, P., Pralle, A., Isacoff, E. Y., Heald, R., and Weis, K. (2006). Analysis of a RanGTP-regulated gradient in mitotic somatic cells. Nature *440*, 697-701.
Kalab, P., Weis, K., and Heald, R. (2002). Visualization of a Ran-GTP gradient in interphase and mitotic Xenopus egg extracts. Science *295*, 2452-2456.
Kapitein, L. C., Peterman, E. J., Kwok, B. H., Kim, J. H., Kapoor, T. M., and Schmidt, C. F. (2005). The bipolar mitotic kinesin Eg5 moves on both microtubules that it crosslinks. Nature *435*, 114-118.
Kapoor, T. M., Mayer, T. U., Coughlin, M. L., and Mitchison, T. J. (2000). Probing spindle assembly mechanisms with monastrol, a small molecule inhibitor of the mitotic kinesin, Eg5. J Cell Biol *150*, 975-988.
Kapoor, T. M., and Mitchison, T. J. (2001). Eg5 is static in bipolar spindles relative to tubulin: evidence for a static spindle matrix. J Cell Biol *154*, 1125-1133.
Karsenti, E., and Vernos, I. (2001). The mitotic spindle: a self-made machine. Science *294*, 543-547.
Kashina, A. S., Baskin, R. J., Cole, D. G., Wedaman, K. P., Saxton, W. M., and Scholey, J. M. (1996a). A bipolar kinesin. Nature *379*, 270-272.
Kashina, A. S., Scholey, J. M., Leszyk, J. D., and Saxton, W. M. (1996b). An essential bipolar mitotic motor. Nature *384*, 225.
King, S. J., and Schroer, T. A. (2000). Dynactin increases the processivity of the cytoplasmic dynein motor. Nat Cell Biol *2*, 20-24.
Koffa, M. D., Casanova, C. M., Santarella, R., Kocher, T., Wilm, M., and Mattaj, I. W. (2006). HURP is part of a Ran-dependent complex involved in spindle formation. Curr Biol *16*, 743-754.

Korneev, M. J., Lakamper, S., and Schmidt, C. F. (2007). Load-dependent release limits the processive stepping of the tetrameric Eg5 motor. Eur Biophys J *36*, 675-681.
Kwok, B. H., Kapitein, L. C., Kim, J. H., Peterman, E. J., Schmidt, C. F., and Kapoor, T. M. (2006). Allosteric inhibition of kinesin-5 modulates its processive directional motility. Nat Chem Biol *2*, 480-485.
Kwok, B. H., and Kapoor, T. M. (2007). Microtubule flux: drivers wanted. Curr Opin Cell Biol *19*, 36-42.
Lawrence, C. J., Dawe, R. K., Christie, K. R., Cleveland, D. W., Dawson, S. C., Endow, S. A., Goldstein, L. S., Goodson, H. V., Hirokawa, N., Howard, J.*, et al.* (2004). A standardized kinesin nomenclature. J Cell Biol *167*, 19-22.
Le Guellec, R., Paris, J., Couturier, A., Roghi, C., and Philippe, M. (1991). Cloning by differential screening of a Xenopus cDNA that encodes a kinesin-related protein. Mol Cell Biol *11*, 3395-3398.
Liao, H., Li, G., and Yen, T. J. (1994). Mitotic regulation of microtubule cross-linking activity of CENP-E kinetochore protein. Science *265*, 394-398.
Lohka, M. J., and Masui, Y. (1984). Roles of cytosol and cytoplasmic particles in nuclear envelope assembly and sperm pronuclear formation in cell-free preparations from amphibian eggs. J Cell Biol *98*, 1222-1230.
Mallik, R., Carter, B. C., Lex, S. A., King, S. J., and Gross, S. P. (2004). Cytoplasmic dynein functions as a gear in response to load. Nature *427*, 649-652.
Mallik, R., and Gross, S. P. (2004). Molecular motors: strategies to get along. Curr Biol *14*, R971-982.
Masui, Y. (1974). A cytostatic factor in amphibian oocytes: its extraction and partial characterization. J Exp Zool *187*, 141-147.
Mayer, T. U., Kapoor, T. M., Haggarty, S. J., King, R. W., Schreiber, S. L., and Mitchison, T. J. (1999). Small molecule inhibitor of mitotic spindle bipolarity identified in a phenotype-based screen. Science *286*, 971-974.
McNally, F. J., and Thomas, S. (1998). Katanin is responsible for the M-phase microtubule-severing activity in Xenopus eggs. Mol Biol Cell *9*, 1847-1861.
McNally, F. J., and Vale, R. D. (1993). Identification of katanin, an ATPase that severs and disassembles stable microtubules. Cell *75*, 419-429.
Mishima, M., Pavicic, V., Gruneberg, U., Nigg, E. A., and Glotzer, M. (2004). Cell cycle regulation of central spindle assembly. Nature *430*, 908-913.
Mitchison, T., and Kirschner, M. (1984). Dynamic instability of microtubule growth. Nature *312*, 237-242.
Mitchison, T. J. (1989). Polewards microtubule flux in the mitotic spindle: evidence from photoactivation of fluorescence. J Cell Biol *109*, 637-652.
Mitchison, T. J., Maddox, P., Groen, A., Cameron, L., Perlman, Z., Ohi, R., Desai, A., Salmon, E. D., and Kapoor, T. M. (2004). Bipolarization and poleward flux correlate during Xenopus extract spindle assembly. Mol Biol Cell *15*, 5603-5615.
Miyamoto, D. T., Perlman, Z. E., Burbank, K. S., Groen, A. C., and Mitchison, T. J. (2004). The kinesin Eg5 drives poleward microtubule flux in Xenopus laevis egg extract spindles. J Cell Biol *167*, 813-818.
Moore, A., and Wordeman, L. (2004). The mechanism, function and regulation of depolymerizing kinesins during mitosis. Trends Cell Biol *14*, 537-546.
Mountain, V., and Compton, D. A. (2000). Dissecting the role of molecular motors in the mitotic spindle. Anat Rec *261*, 14-24.
Mountain, V., Simerly, C., Howard, L., Ando, A., Schatten, G., and Compton, D. A. (1999). The kinesin-related protein, HSET, opposes the activity of Eg5 and cross-links microtubules in the mammalian mitotic spindle. J Cell Biol *147*, 351-366.

Murray, A. W., and Kirschner, M. W. (1989). Cyclin synthesis drives the early embryonic cell cycle. Nature *339*, 275-280.
Murray, A. W., Solomon, M. J., and Kirschner, M. W. (1989). The role of cyclin synthesis and degradation in the control of maturation promoting factor activity. Nature *339*, 280-286.
Rogers, G. C., Rogers, S. L., Schwimmer, T. A., Ems-McClung, S. C., Walczak, C. E., Vale, R. D., Scholey, J. M., and Sharp, D. J. (2004). Two mitotic kinesins cooperate to drive sister chromatid separation during anaphase. Nature *427*, 364-370.
Rogers, G. C., Rogers, S. L., and Sharp, D. J. (2005). Spindle microtubules in flux. J Cell Sci *118*, 1105-1116.
Roghi, C., Giet, R., Uzbekov, R., Morin, N., Chartrain, I., Le Guellec, R., Couturier, A., Doree, M., Philippe, M., and Prigent, C. (1998). The Xenopus protein kinase pEg2 associates with the centrosome in a cell cycle-dependent manner, binds to the spindle microtubules and is involved in bipolar mitotic spindle assembly. J Cell Sci *111 (Pt 5)*, 557-572.
Roof, D. M., Meluh, P. B., and Rose, M. D. (1992). Kinesin-related proteins required for assembly of the mitotic spindle. J Cell Biol *118*, 95-108.
Rosenfeld, S. S., Xing, J., Jefferson, G. M., and King, P. H. (2005). Docking and rolling, a model of how the mitotic motor Eg5 works. J Biol Chem *280*, 35684-35695.
Sablin, E. P., Case, R. B., Dai, S. C., Hart, C. L., Ruby, A., Vale, R. D., and Fletterick, R. J. (1998). Direction determination in the minus-end-directed kinesin motor ncd. Nature *395*, 813-816.
Saunders, A. M., Powers, J., Strome, S., and Saxton, W. M. (2007). Kinesin-5 acts as a brake in anaphase spindle elongation. Curr Biol *17*, R453-454.
Saunders, W. S., and Hoyt, M. A. (1992). Kinesin-related proteins required for structural integrity of the mitotic spindle. Cell *70*, 451-458.
Sawin, K. E., LeGuellec, K., Philippe, M., and Mitchison, T. J. (1992a). Mitotic spindle organization by a plus-end-directed microtubule motor. Nature *359*, 540-543.
Sawin, K. E., and Mitchison, T. J. (1995). Mutations in the kinesin-like protein Eg5 disrupting localization to the mitotic spindle. Proc Natl Acad Sci U S A *92*, 4289-4293.
Sawin, K. E., Mitchison, T. J., and Wordeman, L. G. (1992b). Evidence for kinesin-related proteins in the mitotic apparatus using peptide antibodies. J Cell Sci *101 (Pt 2)*, 303-313.
Scholey, J. M., Rogers, G. C., and Sharp, D. J. (2001). Mitosis, microtubules, and the matrix. J Cell Biol *154*, 261-266.
Schroer, T. A. (1994). Structure, function and regulation of cytoplasmic dynein. Curr Opin Cell Biol *6*, 69-73.
Seitz, A., and Surrey, T. (2006). Processive movement of single kinesins on crowded microtubules visualized using quantum dots. Embo J *25*, 267-277.
Sharp, D. J., McDonald, K. L., Brown, H. M., Matthies, H. J., Walczak, C., Vale, R. D., Mitchison, T. J., and Scholey, J. M. (1999a). The bipolar kinesin, KLP61F, cross-links microtubules within interpolar microtubule bundles of Drosophila embryonic mitotic spindles. J Cell Biol *144*, 125-138.
Sharp, D. J., Rogers, G. C., and Scholey, J. M. (2000). Microtubule motors in mitosis. Nature *407*, 41-47.
Sharp, D. J., Yu, K. R., Sisson, J. C., Sullivan, W., and Scholey, J. M. (1999b). Antagonistic microtubule-sliding motors position mitotic centrosomes in Drosophila early embryos. Nat Cell Biol *1*, 51-54.
Shirasu-Hiza, M., Perlman, Z. E., Wittmann, T., Karsenti, E., and Mitchison, T. J. (2004). Eg5 causes elongation of meiotic spindles when flux-associated microtubule depolymerization is blocked. Curr Biol *14*, 1941-1945.

Silverman-Gavrila, R. V., and Wilde, A. (2006). Ran is required before metaphase for spindle assembly and chromosome alignment and after metaphase for chromosome segregation and spindle midbody organization. Mol Biol Cell *17*, 2069-2080.
Starr, D. A., Williams, B. C., Hays, T. S., and Goldberg, M. L. (1998). ZW10 helps recruit dynactin and dynein to the kinetochore. J Cell Biol *142*, 763-774.
Surrey, T., Nedelec, F., Leibler, S., and Karsenti, E. (2001). Physical properties determining self-organization of motors and microtubules. Science *292*, 1167-1171.
Tsai, M. Y., Wang, S., Heidinger, J. M., Shumaker, D. K., Adam, S. A., Goldman, R. D., and Zheng, Y. (2006). A mitotic lamin B matrix induced by RanGTP required for spindle assembly. Science *311*, 1887-1893.
Tsai, M. Y., Wiese, C., Cao, K., Martin, O., Donovan, P., Ruderman, J., Prigent, C., and Zheng, Y. (2003). A Ran signalling pathway mediated by the mitotic kinase Aurora A in spindle assembly. Nat Cell Biol *5*, 242-248.
Turner, J., Anderson, R., Guo, J., Beraud, C., Fletterick, R., and Sakowicz, R. (2001). Crystal structure of the mitotic spindle kinesin Eg5 reveals a novel conformation of the neck-linker. J Biol Chem *276*, 25496-25502.
Vale, R. D. (1991). Severing of stable microtubules by a mitotically activated protein in Xenopus egg extracts. Cell *64*, 827-839.
Vale, R. D., Reese, T. S., and Sheetz, M. P. (1985). Identification of a novel force-generating protein, kinesin, involved in microtubule-based motility. Cell *42*, 39-50.
Valentine, M. T., Fordyce, P. M., Krzysiak, T. C., Gilbert, S. P., and Block, S. M. (2006). Individual dimers of the mitotic kinesin motor Eg5 step processively and support substantial loads in vitro. Nat Cell Biol *8*, 470-476.
Valentine, M. T., and Gilbert, S. P. (2007). To step or not to step? How biochemistry and mechanics influence processivity in Kinesin and Eg5. Curr Opin Cell Biol *19*, 75-81.
Walczak, C. E., Mitchison, T. J., and Desai, A. (1996). XKCM1: a Xenopus kinesin-related protein that regulates microtubule dynamics during mitotic spindle assembly. Cell *84*, 37-47.
Wilde, A., Lizarraga, S. B., Zhang, L., Wiese, C., Gliksman, N. R., Walczak, C. E., and Zheng, Y. (2001). Ran stimulates spindle assembly by altering microtubule dynamics and the balance of motor activities. Nat Cell Biol *3*, 221-227.
Wittmann, T., and Hyman, T. (1999). Recombinant p50/dynamitin as a tool to examine the role of dynactin in intracellular processes. Methods Cell Biol *61*, 137-143.
Wong, C., and Stearns, T. (2003). Centrosome number is controlled by a centrosome-intrinsic block to reduplication. Nat Cell Biol *5*, 539-544.

7 Appendix

7.1 Résumé

Par cette étude, nous montrons que la phosphorylation d'Eg5 par Eg2 n'est pas importante pour sa fonction dans la formation du fuseau mitotique dans l'extrait d'oeuf de Xénope. Au contraire, la phosphorylation d'Eg5 par Cdk1 est nécessaire pour son attachement aux microtubules. Cet attachement permettra par la suite l'assemblage du fuseau mitotique. En plus de confirmer de précédentes études, ces résultats indiquent que le site de phosphorylation de Cdk1 n'est pas seulement conservé parmi les membres des Kinésines 5, mais également que son mécanisme de régulation est conservé.

Bien que des expériences plus approfondies soient nécessaires afin de caractériser les propriétés motrices d'Eg5 par l'intermédiaire de notre expérience de "microtubule-gliding" dans l'extrait de Xénope, nos expériences réalisées avec des chimères d'Eg5 ont souligné l'importance des propriétés motrices intrinsèques à Eg5 qui sont cruciales pour la formation du fuseau mitotique. En effet, aucune de ces chimères n'a pu rétablir la formation du fuseau mitotique. De plus, ces expériences ont fourni la première preuve expérimentale que la classification des Kinésines en différentes sous-familles selon la conservation de séquence de leur domaine moteur a également abouti à les classer selon leurs différentes fonctions.

7.2 Abstract

In this study, we show that Eg2 phosphorylation of Eg5 is not important for its function in bipolar spindle formation in *Xenopus* egg extract. Conversely, Eg5 needs to be phosphorylated by Cdk1 to be targeted to spindle microtubules and hence assemble a bipolar spindle in *Xenopus* egg extract. These findings confirm previous studies and furthermore indicate that Cdk1 phosphorylation site is not only conserved among kinesin-5 members but also that its mechanism of regulation is conserved among this subfamily.

Although further experiments are required to fully characterize Eg5 motor properties in by means of our microtubule gliding assay in *Xenopus* egg extract, Eg5 intrinsic motor properties are definitely crucial for bipolar spindle assembly as none of the Eg5 chimeras could rescue spindle formation in *Xenopus* egg extract. Moreover, these experiments provide the first experimental evidence that the classification of kinesins in different subfamilies, according to their conserved motor domain sequences, has also yielded to classify them according to their diverse function.

7.3 Abbreviations

AAA	ATPase Associated with diverse cellular Activities
ADP	Adenosine DiPhosphate
ATP	Adenosine TriPhosphate
Cdk	Cyclin dependent kinase
Ci	Curie
CSF	CytoStatic Factor
DNA	DeoxyriboNucleic Acid
e.g.	*exampli gratia*
EDTA	Ethylene Diamine Tetraacetic Acid
EGTA	Ethylene Glycol Tetraacetic Acid
g	gram
GDP	Guanosine DiPhosphate
GFP	Green Fluorescent Protein
GPS	Group-based Phosphorylation Scoring
GST	Glutathione-S-Transferase
GTP	Guanosine TriPhosphate
KRP	Kinesin-Related Protein
l	liter
m	micrometer
M	Molar
m	milli
m	meter
MAP	Microtubule Associated Protein
min	minute
MPF	Mitotis Promoting Factor
MT	MicroTubule
n	nano
N	Newton
NHS	N-HydroxySuccinimide
nRNA	messenger RNA
p	pico

PBS	Phosphate Buffered Saline
PCR	Polymerase Chain Reaction
PEG	PolyEthylene Glycol
pH	potential of Hydrogen
RNA	RiboNucleic Acid
s	second
SDS-PAGE	Sodium Dodecyl Sulfate - Polyacrylamide Gel Electrophoresis
ser	serine
thr	threonine
v/v	by volume
WT	Wild-Type

7.4 Publications

Blümmel, J., Cahu, J., Sandblad, L., Schmitz, C., Surrey, T., and Spatz, J. (2007). Motor Protein Driven Microtubule Transport on Gold Particle Nanopattern, Submitted)